On the Scalability of Cooperative Time Synchronization in Pulse-Connected Networks

An-swol Hu   Sergio D. Servetto

Abstract

The problem of time synchronization in dense wireless networks is considered. Well established synchronization techniques suffer from an inherent scalability problem in that synchronization errors grow with an increasing number of hops across the network. In this work, a model for communication in wireless networks is first developed, and then the model is used to define a new time synchronization mechanism. A salient feature of the proposed method is that, in the regime of asymptotically dense networks, it can average out all random errors and maintain global synchronization in the sense that all nodes in the multi-hop network can see identical timing signals. This is irrespective of the distance separating any two nodes.

Index Terms

Cooperation in networks, large network asymptotics, relay networks, scalability, sensor networks, time synchronization, wireless communications.

I. INTRODUCTION

A. Time Synchronization in Large Distributed Systems

The problem of time synchronization in large distributed systems consists of giving all the physically disjoint elements of the system a common time scale on which to operate. This common time scale is usually achieved by periodically synchronizing the clock at each element to a reference time source, so that the local time seen by each element of the system is approximately the same. Time synchronization plays an important role in many systems in that it allows the entire system to cooperate and function as a cohesive group.

Time synchronization is an old problem [26], but the question of scalability is not. Recent advances in sensor networks show a clear trend towards the development of large scale networks with high node density. For example, a hardware simulation-and-deployment platform for wireless sensor networks capable of simulating networks with on the order of 100,000 nodes was recently developed [24]. As well, for many years the Smart Dust project sought to build cubic-millimeter motes for a wide range of applications [43]. Also, there is work in progress on the drastic miniaturization of power sources [27]. These developments (and many others) indicate that large scale, high density networks are on the horizon.

Large scale, high density networks have applications in a variety of situations. Consider, for example, the military application of sniper localization. Large numbers of wireless nodes can be deployed to find the shooter location as well as the trajectory of the projectile [1]. Since the effective range of a long-range sniper rifle can be nearly 2km, in order to fully track the trajectory of the projectile it may be essential that our deployed network be tightly synchronized over distances of a few kilometers. Another example might be the implementation of a distributed radio for communication. In extracting information from a deployed sensor network, it may be beneficial for the nodes to cooperatively transmit information to a far away receiver [6], [7], [20]. Such an application would require that nodes across the network be well synchronized. As a result, a need for the synchronization of large distributed systems is very real and one that requires careful study to understand the fundamental performance limits on synchronization.

B. Approaches to Synchronization and the Limitations

The synchronization of large networks has been studied in fields ranging from biology to electrical engineering. The study of synchronous behavior has generally taken one of two approaches. The first approach is to consider synchronization as an emergent behavior in complex networks of oscillators. In that work, models are developed to describe natural phenomena and synchronization emerges from these models. The second approach is to develop and analyze algorithms that synchronize engineering networks. Nodes are programmed with algorithms that estimate clock skew and clock offset to achieve network synchronization. However, both of these approaches have significant limitations.

1) The Emergence of Synchronous Behavior: Emergent synchronization properties in large populations has been the object of intense study in the applied mathematics ([30], [41]), physics ([3], [4], [5], [9], [12], [14], [16], [25]), and neural networks ([21], [37]) literature. These studies were motivated by a number of examples observed in nature:

- In certain parts of south-east Asia, thousands of male fireflies congregate in trees and flash in synchrony at night [2].

- Pacemaker cells of the heart, which on average cause 80 contractions a minute during a person's lifetime [22].

- The insulin-secreting cells of the pancreas [35].

For further information and examples, see [32], [40], [31], [42], and the references therein.

A number of models have been proposed to explain the emergence of synchrony, but perhaps one of the most successful and well known is the model of *pulse-coupled oscillators* by Mirollo and Strogatz [32], based on dynamical systems theory. Consider a function $f : [0, 1] \rightarrow [0, 1]$ that is smooth, monotone increasing, concave down (i.e., $f' > 0$ and $f'' < 0$), and is such that $f(0) = 0$ and $f(1) = 1$. Consider also a phase variable ϕ such that $\partial \phi / \partial t = \frac{1}{T}$, where T is the period of a cycle. Then, each element in a group of N oscillators is described by a state variable $x_i \in [0, 1]$ and a phase variable $\phi_i \in [0, 1]$ as follows:

- In isolation, $x_i(t) = f(\phi_i(t))$.

- If $\phi_i(t) = 0$ then $x_i(t) = 0$, and if $\phi_i(t) = 1$ then $x_i(t) = 1$.

- When $x_i(t_0) = 1$ for any of the i's and some time t_0, then for all other $1 \leq j \leq N$, $j \neq i$

$$\phi_j(t_0^+) = \begin{cases} f^{-1}(x_j(\phi_j(t_0)) + \varepsilon_i), & x_j(\phi_j(t_0)) + \varepsilon_i \leq 1 \\ 1, & x_j(\phi_j(t_0)) + \varepsilon_i > 1, \end{cases}$$

where t_0^+ denotes an infinitesimal amount of time after t_0. That is, oscillator i reaching the end of a cycle causes the state of all other oscillators to increase by the amount ε_i, and the phase variable to change accordingly.

The state variable x_i can be thought of as a voltage. Charge is accumulated over time according to the nonlinearity f and it discharges once it reaches full charge, resetting the charging process. Upon discharging, it causes all other charges to increase by a fixed amount of ε_i, up to the discharge point. For this model, it is proved in [32] that for all N and for almost all initial conditions, the system eventually becomes synchronized.

For the network to converge into a synchronous state, one key assumption is that the behavior of every single oscillator is governed by the same function $f(\cdot)$. This means that all oscillators must have the same frequency. From the literature, it appears that this requirement is nearly always needed. As far as we are aware, for a fully synchronous behavior to emerge, the oscillators need to have the same, or nearly the same, oscillation frequencies.

The need for nearly identical oscillators presents a significant limitation for emergent synchronization. This emergence of synchrony is clearly desirable and it has been considered for communication and sensor

networks in [17], [18], [28]. However, whether or not these techniques can be adapted to synchronize networks with nodes that have arbitrary oscillator frequencies (clock skew) is still unclear. Thus, in order to overcome this limitation and find techniques capable of synchronizing a more general class of networks, we turn to algorithms designed to estimate certain unknown parameters such as clock skew.

2) Estimation of Synchronization Parameters and the Scalability Problem: There have been many synchronization techniques proposed for use in sensor networks. These algorithms generally allow each node to estimate its clock skew and clock offset relative to the reference clock. Reference Broadcast Synchronization (RBS) [8] eliminates transmitter side uncertainties by having a transmitter broadcast reference packets to the surrounding nodes. The receiving nodes then synchronize to each other using the arrival of the reference packets as synchronization events. Tiny-Sync/Mini-Sync [36] and the Timing-sync Protocol for Sensor Networks (TPSN) [11] organize the network into a hierarchial structure and the nodes are synchronized using pair-wise synchronization. In lightweight tree-based synchronization (LTS) [13], pair-wise synchronization is also employed but the goal of LTS is to reduce communication and computation requirements by taking advantage of relaxed accuracy constraints. The Flooding Time Synchronization Protocol (FTSP) [29] achieves one-hop synchronization by having a root node broadcast timing information to surrounding nodes. These surrounding nodes then proceed to broadcast their synchronized timing information to nodes beyond the broadcast domain of the root node. This process can continue for multi-hop networks.

The problem with each of these traditional synchronization techniques is that synchronization error will increase with each hop. Since each node is estimating certain synchronization parameters, i.e. clock skew, there will be inherent errors in the estimate. As a result, a node multiple hops away from the node with the reference clock will be estimating its parameters from intermediate nodes that already have estimation errors. Therefore, this introduces a fundamental *scalability problem*: as the number of hops across the network grows, the synchronization error across the network will also grow.

Current trends in network technology are clearly moving us in the direction of large, multi-hop networks. First, sensors are decreasing in size and this size decrease will most likely be accompanied by a decrease in communication range. Thus, more hops will be required to traverse a network deployed over a given area. Second, as we deploy networks over larger and larger areas, then for a given communication range, the number hops across the network will also increase. In either case, the increased number of hops required to communicate across the network will increase synchronization error. Therefore, it is essential that we develop techniques than can mitigate the accumulation of synchronization error over multiple hops.

C. Spatial Averaging and Synchronization

1) Cooperation through Spatial Averaging: To decrease the error increase in each hop, we need to decrease the estimation error. There are two primary ways of achieving this. First, each node can increase the amount of timing information it obtains from neighboring nodes. For example, from a received timing packet, the node may be able to construct a data point telling it the approximate time at the reference clock and the corresponding time at its local clock. Using a collection of these data points, the node can estimate clock skew and clock offset. So instead of using, say, five packets with timing information, a node can wait for ten packets. More data points will generally give better estimates. The drawback to such an approach is the increase in the number of packet exchanges.

The second way in which to reduce estimation error is to increase the quality of each data point obtained by the nodes. This can be achieved through improving packet exchange algorithms and time stamping techniques. However, we believe that there is one fundamentally new approach to improving data point quality that has not be carefully studied. This is to use spatial averaging to improve the quality of each data point.

The motivation for this approach is very simple. Assume that each node has many neighbors. If all nodes in the network are to be synchronized, then the neighbors of any given node will also have synchronization information. Is it possible to simultaneously use information from all the neighbors to improve the quality of a timing observation made by a node? Furthermore, it would seem to make sense that with more neighbors, hence more available timing information, the quality of the constructed data point should improve. If this is indeed the case, then achieving synchronization through the use of spatial averaging will provide a fundamentally new trade-off in improving synchronization performance. Network designers would simply be able to increase the number and density of nodes to obtain better network synchronization. The study of cooperative time synchronization using spatial averaging is the focus of this work.

2) Model and Technique: To obtain a model for developing cooperative synchronization in large wireless networks, we begin by looking at the signals observed by a node in a network with N nodes uniformly deployed over a fixed finite area. To start, we assume propagation delay to negligible (the general case is considered in Section V). All nodes transmit a pulse $p(t)$ and a node j will see a signal $A_{j,N}(t)$ which is the superposition of all these pulses,

$$A_{j,N}(t) = \sum_{i=1}^{N} \frac{A_{max} K_{j,i}}{N} p(t - \tau_0 - T_i).$$

In this expression, $p(t)$ is the basic pulse transmitted by each node (assumed to be the same for all nodes). τ_0 is the ideal pulse transmit time, but since we assume imperfect time synchronization among the nodes we have T_i modelling random errors in the pulse transmission time. $K_{j,i}$ models the amplitude loss in the signal transmitted by the ith node. A_{max} is the maximum magnitude transmitted by a node. We scale each node's transmission by N so that as the network density grows, the total power radiated does not grow unbounded. This model thus describes the received signal seen at a node j for a network with N nodes and this holds for any N. Increasing N will have two effects: (a) node density will increase since the network area is fixed and (b) node signal transmission magnitude will decrease due to the $1/N$ scaling. Therefore, by increasing N this model allows us to study the scalability of networks as node density grows and node size decreases.

Given that these are the signals observed at each node, we ask: is it possible for $A_{j,N}(t)$ to encode a time synchronization signal that will enable all nodes in the network to synchronize their clocks with bounded error, as $N \to \infty$? The answer is yes, and the key to proving all our results is the law of large numbers.

Our key idea is the following. If all nodes were able to determine when time τ_0 (in the reference time) arrives, then by transmitting $p(t)$ at time τ_0, the signal observed at any node j would be $p(t - \tau_0) \sum_{i=1}^{N} \frac{A_{max} K_{j,i}}{N}$, which is a suitably scaled version of $p(t)$ centered at τ_0. In reality however, there will be some error in the determination of τ_0, which we account for by allowing for a node-dependent random error T_i. But, if the distribution of T_i satisfies certain conditions, then the effects of that timing error can be averaged out. A pictorial representation of why this should be the case is shown in Fig. 1.
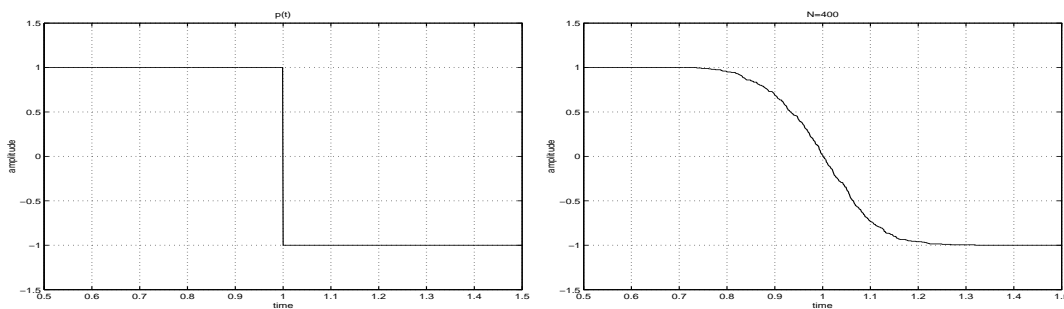

Fig. 1.   Assume N square waves are transmitted (one by each node) at random times. These times have the properties that they all have the same mean, a small variance compared to the duration of the wave, and their distribution is symmetric. Then, under the assumption of N large, it follows from the Law of Large Numbers that the observed signal is going to be a smoothed version of the square wave, in which the center *zero-crossing* will correspond to the location of the mean of the random times.

Therefore, intuitively we can see how the technique of *cooperative time synchronization* using spatial averaging can average out the inherent timing errors in each node. Even though there is randomness and uncertainty in each node's estimates, by using cooperation among a large number of nodes it is possible to recover *deterministic* parameters from the resulting aggregate waveform (such as the location of certain zero-crossings) in the limit as node density grows unbounded. Thus more nodes will give us better estimates. This is because the random waveform converges to a deterministic one as more and more nodes cooperatively generate an aggregate waveform. At the same time, the average power required by each node will decrease since smaller nodes send smaller signals. Therefore, by programming suitable dynamics into the nodes, in this paper we show how it is possible to generate an aggregate output signal with *equispaced* zero-crossings in the limit of asymptotically dense networks. Thus, the detection of these zero-crossings plays the same role as that of an externally generated time reference signal based on which all nodes can synchronize.

We develop this synchronization technique in three main steps. One, we set up the model for $A_{j,N}(t)$. Two, we specify characteristics of the model (i.e. the distribution of T_i) that allow us to prove desirable properties of the aggregate waveform (such as a center zero-crossing at τ_0). Three, we develop the estimators needed for our synchronization technique and show that the estimators give us the desired characteristics.

D. Main Contributions and Organization of the Paper

The main contributions presented in this paper are the following;

- The definition of a probabilistic model for the study of the time synchronization problem in wireless networks. This model does contain the classical Mirollo-Strogatz model as a special case, but its formulation and the tools used to prove convergence results are of a completely different nature (purely probabilistic, instead of based on the theory of dynamical systems).

- Using this model, we provide a rigorous analysis of a new cooperative time synchronization technique that employs spatial averaging and has favorable scaling properties. As the density of nodes increases, synchronization performance improves. In particular, in the limit of infinite density, deterministic parameters for synchronization can be recovered.

- We show that cooperative time synchronization works perfectly for negligible propagation delay. When propagation delay is considered, we find that asymmetries at the boundaries reveal some limitations that need to be carefully considered in designing algorithms that take advantage of spatial averaging.

In analyzing the proposed cooperative time synchronization technique, our goal is to show that the proposed technique can average out all random error and provide deterministic parameters for synchronization as node density grows unbounded. This asymptotic result can be viewed as a *convergence in scale* to synchrony. The result serves as a theoretical foundation for allowing a new trade-off between node density and synchronization performance. In particular, higher node density can yield better synchronization.

The rest of this paper is organized as follows. The general model is presented in Section II. Of particular interest here is Section II-E, where we show how our model contains the model of Mirollo and Strogatz for pulse-coupled oscillators as a special case [32]. In Section III we specialize the general model for our synchronization setup and develop waveform properties that will be used in time synchronization. In Section IV we develop the cooperative time synchronization technique for no propagation delay. We extend the cooperative synchronization ideas to the case of propagation delay in Section V. The paper concludes in Section VI with a detailed discussion on the scalability issue and how the technique proposed in this work lays the theoretical foundation for a general class of cooperative time synchronization techniques that use spatial averaging.

II. SYSTEM MODEL

A. Clock Model

We consider a network with N nodes uniformly distributed over a fixed finite area. The behavior of each node i is governed by a clock c_i that counts up from 0. The introduction of c_i is important since it provides a consistent timescale for node i. By maintaining a table of pulse-arrival times, node i can utilize the arrival times of many pulses over an extended period of time.

The clock of one particular node in the network will serve as the reference time and to this clock we wish to synchronize all other nodes. We will call the node with the reference clock node 1 and the clocks of other nodes are defined relative to the clock of node 1. We never adjust the frequency or offset of the local clock c_i because we wish to maintain a consistent time scale for node i.

The clock of node 1, c_1, will be defined as $c_1(t) = t$ where $t \in [0, \infty)$. Taking c_1 to be the reference clock, we now define the clock of any other arbitrary node i, c_i. We define c_i as

$$c_i(t) = \alpha_i(t - \bar{\Delta}_i) + \Psi_i(t), \tag{1}$$

where

- $\bar{\Delta}_i$ is an unknown offset between the start times of c_i and c_1.

- $\alpha_i > 0$ is a constant and for each i, $\alpha_i \in [\alpha_{low}, \alpha_{up}]$ where $\alpha_{up}, \alpha_{low} > 0$ are finite. This bound on α_i means that the frequency offsets between any two nodes can not be arbitrarily large.

- $\Psi_i(t)$ is a stochastic process modeling random timing jitter.

Thus, this model assumes that there is a bounded constant frequency offset between the oscillators of any two nodes as well as some random clock jitter.

It is important to note that node 1 does not have to be special in any way; its clock is simply a reference time on which to define the clocks of the other nodes. This means that our clock model actually describes the relative relationship of all the clocks in the network by using an arbitrary node's clock as a reference.

B. Pathloss Only Model

1) A Random Model for Pathloss: From Section I-C.2, we see that we are interested in studying the aggregate waveform observed at a node j. As a result, we are only concerned with the aggregate signal magnitude and do not care about the particular signal contribution from each surrounding node. With this in mind, we can develop a random model for pathloss that, for dense networks, gives the appropriate aggregate signal magnitude at node j. Such a model is ideal for our situation since we are studying asymptotically dense networks.

We start with a general pathloss model $K(d)$, where $0 \leq K(d) \leq 1$ for all distances $d \geq 0$, is non-increasing and continuous. $K(d)$ is a fraction of the transmitted magnitude seen at distance d from the transmitter. For example, if the receiver node j is at distance d from node i, and node i transmits a signal of magnitude A, then node j will hear a signal of magnitude $AK(d)$. We derive $K(d)$ from a power pathloss model since any pathloss model captures the *average* received power at a given distance from the transmitter. This average received power is perfect for modelling received signal magnitudes in our problem setup since we are considering asymptotically dense networks. Due to the large number of nodes at any given distance d from the receiver, using the average received magnitude at distance d as the contribution from each node at that distance will give a good modelling of the amplitude of the aggregate waveform.

The random pathloss variable K_j will be derived from $K(d)$. To understand how K_j and $K(d)$ are related, we give an intuitive explanation of the meaning of K_j as follows: the $\Pr[K_j \in (k, k + \Delta)]$ is the fraction of nodes at distances d from node j such that $K(d) \in (k, k + \Delta)$, where Δ is a small constant. This means that, roughly speaking, for any given scaling factor $K_j = k$, $f_{K_j}(k)\Delta$ is the fraction of received signals with magnitude scaled by approximately k, where $f_{K_j}(k)$ is the probability density function of K_j. Thus, if we scale the transmit magnitude A from every node i by an independent K_j,

then as the number of nodes, N, gets large, node j will see $N f_{K_j}(k)\Delta$ signals of approximate magnitude Ak, and this holds for all k in the range of K_j. This is because taking a large number of independent samples from a distribution results in a good approximation of the distribution.

Thus, this intuition tells us that scaling the magnitude of the signal transmitted from every node i by an independent sample of the random variable K_j gives an aggregate signal at node j that is the same magnitude as if we generated the signal using $K(d)$ directly. Even though the signals from two nodes at the same distance from a receiver have correlated magnitudes, we do not care about the signal magnitude from any particular node but only that an appropriate number of all possible received signal magnitudes contribute to the aggregate waveform. For a receiving node j, we choose therefore to work with the random variable K_j instead of directly with $K(d)$ because, for the goals of this paper, doing so has two major advantages: (a) we can obtain desirable limit results by placing very minimal restrictions on the distribution of the K_j's (and hence on $K(d)$) and (b) we can apply tools from probability theory (basically, the strong law of large numbers) to carry out our analysis.

2) Definition of K_j: From the above intuition we can define the cumulative distribution function of K_j as

$$F_{K_j}(k) \;=\; \Pr(K_j \leq k) \;=\; \begin{cases} 0 & k \in (-\infty, 0) \\ \frac{A_T - A(j,\bar{r})}{A_T} \;=\; 1 - \frac{A(j,\bar{r})}{A_T} & k \in [0,1] \\ 1 & k \in (1,\infty) \end{cases} \qquad (2)$$

where

- A_T is the total area of the network,
- $A(j,a)$ is the area of the network contained in a circle of radius a centered at node j,
- $\bar{r} = \sup\{d : K(d) > k\}$.

From the above discussion we see that the distribution of K_j is only a function of node j, the receiving node. We illustrate the relationship among node j, $K(d)$, $\bar{r}$, and $F_{K_j}(k)$ in Fig 2. We sometimes write $K_{j,i}$ with i used to index each node surrounding node j. i is thus indexing a sequence of independent random variables $K_{j,i}$ for fixed j. Therefore, for a given j, $K_{j,i}$'s are independent and identically distributed (i.i.d.) with a cumulative distribution function given by (2) for all i.

We assume that K_j has the following properties:

- K_j is independent from $\Psi_l(t)$ for all j, l, and t.
- $0 \leq K_j \leq 1$, $0 < E(K_j) \leq 1$, and $\mathrm{Var}(K_j) \leq 1$.

The requirements on the random variable K_j places restrictions on the model $K(d)$. Any function $K(d)$ that yields a K_j with the above requirements can be used to model pathloss.

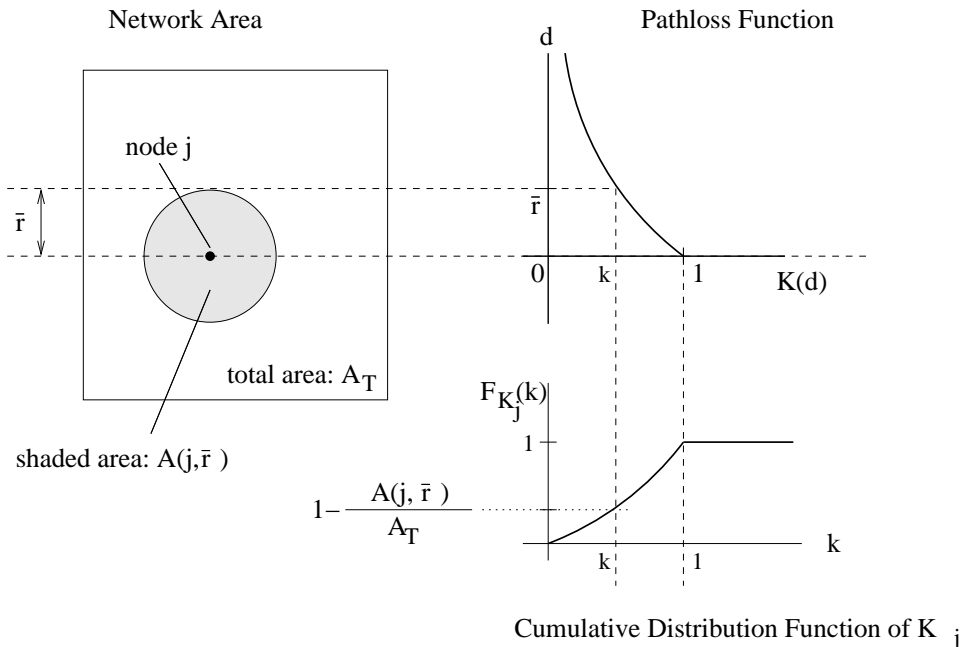Network Area   Pathloss Function

Fig. 2.   An illustration of the cumulative distribution function $F_{K_j}(k)$ is shown in the bottom-right figure. For a given scaling value k, $F_{K_j}(k)$ is defined to be $1 - (A(j,\bar{r})/A_T)$, where the relationship between $\bar{r}$ and k is shown in the top-right figure. The area $A(j,\bar{r})$ and its relation to node j is shown in the top-left figure.

C. Delay and Pathloss Model

In this section we develop a more complex model to simultaneously model propagation delay and pathloss. This leads to the joint development of the delay random variable D_j and a corresponding pathloss random variable K_j.

1) Correlation Between Delay and Pathloss: Since we want to develop a model for both pathloss and time delay, we start by keeping the pathloss function $K(d)$ defined in Section II-B. The general delay model assumes a function $\delta(d)$ that models the time delay as a function of distance. $\delta(d)$ describes the time in terms of c_1 that it takes for a signal to propagate a distance d. For example, if node i and node j are distance d_0 apart, then a pulse sent by node i at time $c_1 = 0$ will be seen at node j at time $c_1 = \delta(d_0)$. We make the reasonable assumption that $\delta(d)$ is continuous and strictly monotonically increasing for $d \geq 0$.

As with the pathloss only model, we want to define a delay random variable D_j for each receiving node j. Recall that this means that for every node j there is a random variable D_j associated with it since, in general, each node j will see different delays. There is a correlation between the delay random

variable D_j and the pathloss random variable K_j. This correlation arises for two main reasons. First, since in Section II-B we define $K(d)$ to be monotonically decreasing and continuous, it is possible for $K(d) = 0$ for $d \in [R, \infty)$, $R > 0$. This might be the case for a multi-hop network. In this situation, there will be a set of nodes whose transmissions will never reach node j (i.e. infinite delay) even though according to $\delta(d)$ these nodes should contribute a signal with finite delay. Second, a small K_j value would represent a signal from a far away node. As a result, the corresponding D_j value should be large to reflect large delay. Therefore, keeping these two points in mind, we proceed to develop a model for both pathloss and propagation delay.

2) Definition of D_j and K_j: We define the cumulative distribution function of D_j as

$$F_{D_j}(x) = \Pr(D_j \leq x) = \begin{cases} 0 & x \in (-\infty, 0) \\ \frac{A(j,r')}{A_T} & x \in [0, \delta(R)] \\ a(x - \delta(R)) + \frac{A(j,R)}{A_T} & x \in (\delta(R), \delta(R + \Delta R)] \\ 1 & x \in (\delta(R + \Delta R), \infty) \end{cases} \tag{3}$$

where $r' = \sup\{r : \delta(r) \leq x\}$, $\Delta R > 0$ is a constant, $R = \sup\{d : K(d) > 0\}$, and

$$a = \frac{1 - \frac{A(j,R)}{A_T}}{\delta(R + \Delta R) - \delta(R)}.$$

Recall that $A(j,a)$, defined in Section II-B, is the area of the network contained in a circle of radius a centered at node j and A_T is the total area of the network. Note that R can be infinite.

Using the delay random variable D_j with the cumulative distribution function in (3), we define K_j as

$$K_j = K(\delta^{-1}(D_j)), \tag{4}$$

where $K(\cdot)$ is the deterministic pathloss function from Section II-B and $\delta^{-1} : [0, \infty) \to [0, \infty)$ is the inverse function of the deterministic delay function $\delta(\cdot)$. Note that $\delta^{-1}(\cdot)$ exists since $\delta(\cdot)$ is continuous and strictly monotonically increasing on $[0, \infty)$.

3) Intuition Behind D_j and K_j: To understand the distribution of D_j, we need to consider the definition of K_j as well. Recall that a signal arriving with delay D_j is scaled by the pathloss random variable K_j. Let us consider the cumulative distribution in two pieces, $x \in [0, \delta(R)]$ and $x \in (\delta(R), \infty)$. The case for $x \in (-\infty, 0)$ is trivial. First, for $x \in [0, \delta(R)]$, the probability that D_j takes a value less than or equal to x is simply the fraction of the network area around node j such that the nodes are at distances d with $\delta(d) \leq x$. The intuition is the same as that for the development of K_j in Section II-B. Second, for $x \in (\delta(R), \infty)$, the situation is more complex. Note that a transmitted signal from a node at distance $d \in (R, \infty)$ from j will arrive at node j with infinite delay since $K(d) = 0$ for $d \in (R, \infty)$. Since any

delay values in $x \in (\delta(R), \infty)$ correspond to distances $d = \delta^{-1}(x) \in (R, \infty)$, the corresponding scaling value will be zero because K_j and D_j are related by (4). As a result, it does not matter what delay values we assign to the fraction of the network area outside a circle of radius R centered at node j as long as their delay value x is such that $\delta^{-1}(x) \in (R, \infty)$. Thus, we can arbitrarily choose a constant ΔR value and construct a piecewise linear portion of the cumulative distribution function of D_j on $x \in (\delta(R), \infty)$. The probability that $D_j \in (\delta(R), \infty)$ will be the fraction of the network area outside a circle of radius R around node j. And since $D_j \in (\delta(R), \infty)$ will have a corresponding K_j value that is zero, this fraction of nodes will not contribute to the aggregate waveform at node j. It is clear that the correlated D_j and K_j random variables work together to accurately model a signal arriving with both pathloss and propagation delay. An illustration of how $K(d)$, $\delta(d)$, node j, and $F_{D_j}(x)$ are related can be found in Fig. 3.
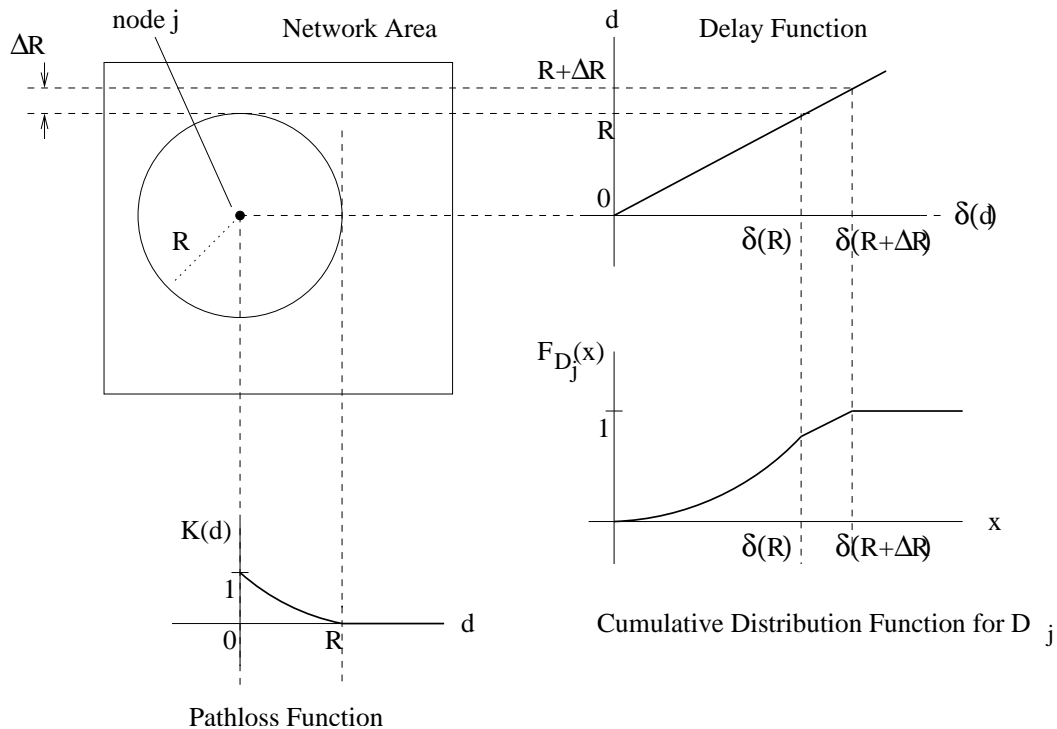

Fig. 3. From the top-left and bottom-left figures, we can see how $K(d)$ determines the set of nodes surrounding node j that will contribute to the aggregate waveform at node j. This contributing set of nodes is related to $F_{D_j}(x)$ through $\delta(d)$ and this is illustrated in the top-right and bottom-right figures.

We require that D_j is bounded, has finite expectation, and has finite variance for all j. Note that $D_j \geq 0$ by the requirement that $\delta(d) \geq 0$. As well, since the cumulative distribution in (3) is continuous, and often absolutely continuous, we assume that D_j has a probability density function $f_{D_j}(x)$. When we

write $D_{j,i}$, the i indexes each node surrounding node j. Thus, the $D_{j,i}$'s are independent and identically distributed in i for a given j and have a cumulative distribution given by (3). Using the K_j and D_j developed in this section to simultaneously model pathloss and propagation delay, respectively, we will be able to closely approximate the received aggregate waveform at any node j as $N \to \infty$.

To summarize, we see that our choice of the pathloss and delay random variables will depend on what we want to model. If we only consider pathloss and not propagation delay, then we will use the random variable K_j defined in Section II-B. If we account for both pathloss and delay, then we will use the delay random variable D_j in this section (Section II-C) and the pathloss random variable K_j defined by (4).

D. Synchronization Pulses and the Pulse-Connection Function

The exchange of pulses is the method through which the network will maintain time synchronization. Each node i will periodically transmit a scaled pulse $A_i p(t)$, where A_i is a constant and $p(t)$, in general, can be any pulse. We call the interval of time during which a synchronization pulse is transmitted a *synchronization phase*.

What each node does with a set of pulse arrival observations is determined by the pulse-connection function $X_{n,i}^{c_i}$ for node i. The pulse-connection function is a function that determines the time, in the time scale of c_i, when node i will send its nth pulse. It can be a function of the current value of $c_i(t)$ and past pulse arrival times. This function basically determines how any node i reacts to the arrival of a pulse.

E. An Example: Pulse-Coupled Oscillators

The system model that we presented thus far is powerful because it is very general. In this section we show that it is a generalization of the pulse-coupled oscillator model proposed by Mirollo and Strogatz [32]. As a result, the results presented in that paper will hold under the simplified version of our model.

1) Model Parameters for Pulse-Coupled Oscillators: In setting up the system model, Mirollo and Strogatz make four key assumptions:

- Pathloss Model: The first assumption that is made is that there is all-to-all coupling among all N oscillators. This means that each oscillator's transmission can be heard by all other oscillators. Thus, for our model we ignore pathloss, i.e. $K(d) = 1$, to allow any node's transmission to be heard by each of the other $N - 1$ nodes.

- Delay Model: The second assumption is that there is instantaneous coupling. This assumption is the same as setting $\delta(d) = 0$. In such a situation we would use our pathloss only model.

- Synchronization Pulses: The third key assumption made in [32] is that there is non-uniform coupling, meaning that each of the N oscillators fire with strengths $\epsilon_1, \ldots, \epsilon_N$. We modify the parameters in our model by making node i transmit with magnitude $A_i = \epsilon_i$. They also assume that any two pulses transmitted at different times will be seen by an oscillator as two separate pulses. In our model, we may choose any pulse $p(t)$ that has an arbitrarily short duration and each node will detect the pulse arrival time and pulse magnitude.

- Clock Model: The fourth important assumption made by Mirollo and Strogatz is that the oscillators are identical but they start in arbitrary initial conditions. We simplify our clock model in (1) by eliminating any timing jitter, i.e. $\Psi_i(t) = 0$, and making the clocks identical by setting $\alpha_i = 1$ for $i = 1, \ldots, N$. We leave $\bar{\Delta}_i$ in the model to account for the arbitrary initial conditions. We also assume that the phase variable in the pulse-coupled oscillator model increases at the same rate as our clock. That is, the time it takes the phase variable to go from zero to one and the time it takes our clock to count from one integer value to the next are the same.

Now that we have identical system models, what remains is to modify our model to mimic the coupling action detailed in [32]. This is accomplished by defining a proper pulse-connection function $X_{n,i}^{c_i}$.

2) Choice of Pulse-Connection Function: To match the coupling action in [32], we choose a pulse transmit time function $X_{n,i}^{c_i}(z_{k,i}^{c_i}, z_{k-1,i}^{c_i}, \ldots, z_{1,i}^{c_i}, x_{n-1,i}^{c_i})$ that is a function of pulse receive times and also the time of node i's $(n-1)$th pulse transmission time. $z_{k,i}^{c_i}$ is the time in terms of c_i that node i receives its kth pulse since its last pulse transmission at $x_{n-1,i}^{c_i}$. In this case, $X_{n,i}^{c_i}$ will be a function that updates node i's nth pulse transmission time each time node i receives a pulse. Let $X_{n,i}^{c_i}(k) \triangleq X_{n,i}^{c_i}(z_{k,i}^{c_i}, z_{k-1,i}^{c_i}, \ldots, z_{1,i}^{c_i}, x_{n-1,i}^{c_i})$ where it is node i's nth pulse transmission time after observing k pulses since its last pulse transmission. Node i will transmit its pulse as soon as $X_{n,i}^{c_i} \leq c_i(t)$ where $c_i(t)$ is node i's current time. As soon as the node transmits a pulse at $X_{n,i}^{c_i}$ the function will reset and become $X_{n+1,i}^{c_i}(0) = x_{n,i}^{c_i} + 1$. The node is now ready to receive pulses and at its first received pulse, the next transmission time will become $X_{n+1,i}^{c_i}(1)$. $X_{n,i}^{c_i}$ will thus be defined as

$$X_{n,i}^{c_i}(k) = X_{n,i}^{c_i}(k-1) - [f^{-1}(\epsilon_j + f(z_{k,i}^{c_i} - x_{n-1,i}^{c_i})) - (z_{k,i}^{c_i} - x_{n-1,i}^{c_i})], \qquad k > 0 \qquad (5)$$

$$X_{n,i}^{c_i}(0) = x_{n-1,i}^{c_i} + 1 \qquad (6)$$

where the pulse received at $z_{k,i}^{c_i}$ is a pulse of magnitude ϵ_j and the function $f : [0,1] \to [0,1]$ is the smooth, monotonic increasing, and concave down function defined in [32].

Equations (5) and (6) fundamentally say that each time node i receives a pulse, node i's next transmission time will be adjusted. This is in line with the behavior of the coupling model described by Mirollo and Strogatz since each time an oscillator receives a pulse, its state variable is pulled up by ϵ thus adjusting the time at which the oscillator will next fire. To see how equations (5) and (6) relate to the coupling model in [32], let us consider an example with two pulse coupled oscillators. Consider two oscillators A and B illustrated in Fig. 4. In Fig. 4(a), we have that oscillator A is at phase q and
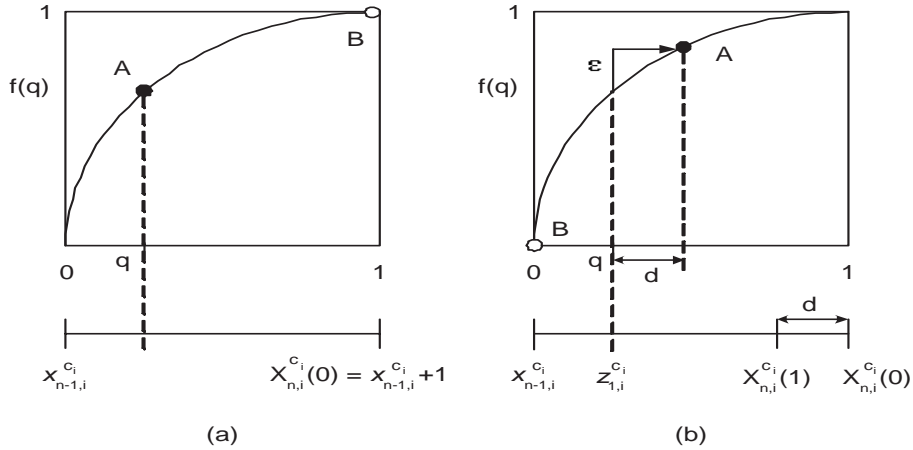

Fig. 4. We illustrate the connection between the pulse-coupled oscillator coupling model and our clock model. In (a), oscillator B is just about to fire and oscillator A has phase q. In (b), oscillator B fires and increases the phase of oscillator A by d. This d increase in phase effectively decreases the time at which A will next fire. We capture this time decrease by decreasing the firing time of our node by an amount d. Thus, oscillator A and our node will fire at the same time.

oscillator B is just about to fire. Below the pulse-coupled oscillator model we have a time axis for node i corresponding to our clock model going from time $x_{n-1,i}^{c_i}$ to $x_{n-1,i}^{c_i} + 1$. Our time axis for node i models the behavior of oscillator A, that is, we want node i to behave in the same way as oscillator A under the influence of oscillator B. If oscillator B did not exist, then the phase variable q will match our clock in that q reaches 1 at the same time our clock reaches $X_{n,i}^{c_i}(0) = x_{n-1,i}^{c_i} + 1$ and oscillator A will fire at the same time our model fires. In Fig. 4(b), oscillator B has fired and has pulled the state variable of oscillator A up by ϵ. This coupling has effectively pushed the phase of oscillator A to $q+d$ and decreased the time before A fires. In fact, the time until oscillator A fires again is decreased by d. We can capture this coupling in our model since we can calculate the lost time d. The time at which oscillator B fires is $z_{1,i}^{c_i}$ and it is clear that $d = f^{-1}(\epsilon + f(z_{1,i}^{c_i} - x_{n-1,i}^{c_i})) - (z_{1,i}^{c_i} - x_{n-1,i}^{c_i})$. Thus, if the time that oscillator A will fire again is decreased by time d due to the pulse of B, then we adjust our node firing time by

decreasing the firing time to $X_{n,i}^{c_i}(1) = x_{n-1,i}^{c_i} + 1 - d$. This is exactly the expression in (5) for $k = 1$. This relationship between our model for calculating the node firing time and the pulse-coupled oscillator coupling model can be easily extended to N oscillators.

We can see then that the pulse-coupled oscillator model proposed by Mirollo and Strogatz in [32] is a special case of our model. Our model generalizes this pulse-coupled oscillator model by considering timing jitter, pulses of finite width, propagation delay, non-identical clocks, and an ability to accommodate arbitrary coupling functions.

III. COOPERATIVE TIME SYNCHRONIZATION SETUP

Just as we could specialize our model to the pulse-coupled oscillator model of Mirollo and Strogatz, we now specialize the model for our proposed synchronization technique. We start under the assumption of no propagation delay and develop the synchronization technique for this case. Propagation delay is considered in Section V. We proceed in three steps. In Section III-B, we specify the model for $A_{j,N}^{c_1}(t)$, the received waveform at any node j. Second, in Section III-C, we prove that given certain characteristics of the model, $A_{j,N}^{c_1}(t)$ has very useful limiting properties. Third, we show in Section IV that estimators (i.e., the pulse connection function) developed for our synchronization technique give $A_{j,N}^{c_1}(t)$ the desired properties.

A. System Parameters

For our synchronization technique, we specialize the general model by making the following assumptions on α_i and $\Psi_i(t)$ for $i = 1 \ldots N$:

- A characterization of the $\{\alpha_i\}$ is given by a known function $f_\alpha(s)$ with $s \in [\alpha_{low}, \alpha_{up}]$ that gives the percentage of nodes with any given α value. Thus, the fraction of nodes with α values in the range s_0 to s_1 can be found by integrating $f_\alpha(s)$ from s_0 to s_1. We assume that $|f_\alpha(s)| < G_\alpha$, for some constant G_α. We keep this function constant as we increase the number of nodes in the network ($N \to \infty$). Given any circle of radius R that intersects the network, the nodes within that circle will have α_i's that are characterized by $f_\alpha(s)$. R is the maximum d such that $K(d) > 0$. This means that the set of nodes that any node j will hear from will have its α_i's characterized by a known function. Note that R can be infinite, and in that case, any node j hears from all nodes in the network. Fundamentally, $f_\alpha(s)$ means that as we increase node density, the new nodes have α parameters that are well distributed in a predictable manner.

- $\Psi_i(t)$ is a zero mean Gaussian process with samples $\Psi_i(t_0) \sim \mathcal{N}(0, \sigma^2)$, for any t_0, and independent and identically distributed samples for any set of times $[t_0, \ldots, t_k]$, k a positive integer. We assume $\sigma^2 < \infty$ and note that σ^2 is defined in terms of the clock of node i. We assume that $\Psi_i(t)$ is Gaussian since the RMS (root mean square) jitter is characterized by the Gaussian distribution [34].

We maintain the full generality of the pathloss model from Section II-B. Note that throughout this work we assume no transmission delay or time-stamping error. This means that a pulse is transmitted at exactly the time the node intends to transmit it. We make this assumption since there will be no delay in message construction or access time [8] because our nodes broadcast the same simple pulse without worrying about collisions. Also, when a node receives a pulse it can determine its clock reading without delay since any time stamping error is small and can be absorbed into the random jitter.

B. Signal Reception Model

For our proposed synchronization technique, the aggregate waveform seen by node j at any time t is

$$A_{j,N}^{c_1}(t) = \sum_{i=1}^{N} \frac{A_{max} K_{j,i}}{N} p(t - \tau_o - T_i), \tag{7}$$

where $A_{j,N}^{c_1}(t)$ is the waveform seen at node j written in the time scale of c_1 and $A_i = A_{max}/N$ for all i. A_{max} is the maximum transmit magnitude of a node. T_i is the random timing offset suffered by the ith node, which encompasses the random clock jitter and estimation error. This model says that each node i's pulse transmission occurs at the ideal transmit time τ_0 plus some random error T_i. In the next section, Section III-C, we find properties for T_i that will give us desirable properties in $A_{j,N}^{c_1}(t)$. Then, in Section IV, we show that our proposed steady-state synchronization technique and its associated pulse-connection function will give us the desired properties.

There are two comments about (7) that we want to make. First, note that even though we sum the transmissions from all N nodes in (7), we do not assume that node j can hear all nodes in the network. Recall from the pathloss model that if we have a multi-hop network, then there will be a nonzero probability that $K_{j,i} = 0$. Thus, node j will not hear from the nodes whose transmissions have zero magnitude. Second, it may be possible that the nodes are told that there are $\bar{N} = vN$ nodes in the network while the actual number of functioning nodes is N. In which case, each node will transmit with signal magnitude $A_i = A_{max}/(vN)$ and (7) will have a factor of $1/v$. Other than for this factor, however, the theoretical results that follow are not affected.

To model the quality of the reception of $A_{j,N}^{c_1}(t)$ by node j, we model the reception of a signal by defining a threshold γ. γ is the received signal threshold required for nodes to perfectly resolve the pulse

arrival time. If the maximum received signal magnitude is less than γ then the node does not make any observations and ignores the received signal waveform. We assume that $\gamma \ll A_{max}$.

In our work we will assume that $p(t)$ takes on the shape

$$p(t) = \begin{cases} q(t) & -\tau_{nz} < t < 0 \\ 0 & t = 0, t \leq -\tau_{nz}, t \geq \tau_{nz} \\ -q(-t) & 0 < t < \tau_{nz} \end{cases} \tag{8}$$

where $\tau_{nz} > 0$ is expressed in terms of c_1. We assume $q(t) > 0$ for $t \in (-\tau_{nz}, 0)$, $q(t) \neq 0$ only on $t \in (-\tau_{nz}, 0)$, $\sup_t |q(t)| = 1$, and $q(t)$ is uniformly continuous on $(-\tau_{nz}, 0)$. Thus, we see that $p(t)$ has at most three jump discontinuities (at $t = 0, -\tau_{nz}, \tau_{nz}$). τ_{nz} should be chosen large compared to $\max_i \sigma_i^2$, i.e. $\sigma_i^2 << \tau_{nz}$, where σ_i^2 is the value of σ^2 translated from the time scale of c_i to c_1. This way, over each synchronization phase, with high probability a zero-crossing will occur. For each node, the duration in terms of c_1 of a synchronization phase will be $2\tau_{nz}$. Note that we assume τ_{nz} is a value that is constant in any consistent time scale. This means that even though nodes have different clocks, identical pulses are transmitted by all nodes. We define a pulse to be transmitted at time t if the pulse makes a zero-crossing at time t. Similarly, we define the *pulse receive (arrival) time* for a node as the time when the observed waveform first makes a zero-crossing. A *zero-crossing* is defined for signals that have a positive amplitude and then transition to a negative amplitude. It is the time that the signal first reaches zero.

For the exchange of synchronization pulses, we assume that nodes can transmit pulses and receive signals at the same time. This simplifying assumption is not required for the ideas presented here to hold, but simplifies the presentation. We mention a way to relax this assumption in Section IV-D.1.

In (7) and in the discussions above, we have focused on characterizing the aggregate waveform for any one synchronization phase. That is, (7) is the waveform seen by any node j for the synchronization phase centered around node 1's transmission at $t = \tau_0$, τ_0 a positive integer. We can, however, describe a synchronization pulse train in the following form,

$$\bar{A}_{j,N}^{c_1}(t) = \sum_{u=1}^{\infty} \sum_{i=1}^{N} \frac{A_{max} K_{j,i}}{N} p(t - \tau_u - T_{i,u}), \tag{9}$$

where τ_u is the integer value of t at the uth synchronization phase, and $T_{i,u}$ is the error suffered by the ith node in the uth synchronization phase. We seek to create this pulse train with equispaced zero-crossings and use each zero-crossing as a synchronization event. An illustration of such a pulse train is shown in Fig. 5. For simplicity, however, most of the theoretical work is carried out on one synchronization phase.
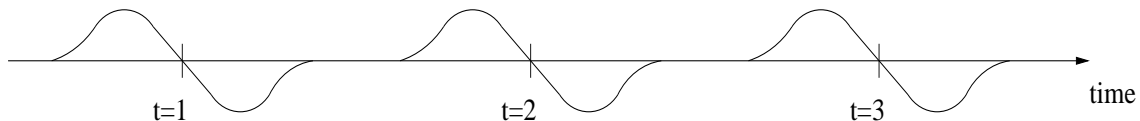
Fig. 5. An illustration of a pulse train with equispaced zero-crossings. The pulse at each integer value of t is an instance of $A_{j,\infty}(t) = \lim_{N \to \infty} A_{j,N}^{c_1}(t)$ so we see three instances of $A_{j,\infty}(t)$ in the above figure with zero-crossings at $t = 1, 2, 3$. We can control the zero-crossings of $A_{j,\infty}(t)$ and choose to place it on an integer value of t. As a result, we can use these zero-crossings as synchronization events since they can be detected simultaneously by all nodes in the network.

C. Desired Structural Properties of the Received Signal

In this section, we characterize the properties of T_i that give us desirable properties in the aggregate waveform. From (7), the aggregate waveform seen at each node j in the network has the form

$$A_N(t) = \frac{1}{N} \sum_{i=1}^{N} A_{max} K_i p(t - \tau_0 - T_i) \tag{10}$$

We have dropped the j and c_1 for notational simplicity since in this section we deal solely with the received waveform at a node j in the time scale of c_1. As we let the number of nodes grow unbounded ($N \to \infty$), the properties of this limit waveform can be characterized by Theorem 1. These properties will be essential for asymptotic cooperative time synchronization. As a note, in Theorem 1 we present the case for Gaussian distributed T_i but similar results hold for arbitrary zero-mean, symmetrically distributed T_i with finite variance.

Theorem 1: Let $p(t)$ be as defined in equation (8) and $T_i \sim \mathcal{N}(0, \frac{\bar{\sigma}^2}{\alpha_i^2})$ with $\bar{\sigma}^2 > 0$ a constant and $\frac{\bar{\sigma}^2}{\alpha_i^2} < B < \infty$ for all i, B a constant. Also, let K_i be defined as in Section II-B and be independent from T_i for all i. Then, $\lim_{N \to \infty} A_N(t) = A_\infty(t)$ has the properties

- $A_\infty(\tau_0) = 0$,
- $A_\infty(t) > 0$ for $t \in (\tau_0 - \tau, \tau_0)$, and $A_\infty(t) < 0$ for $t \in (\tau_0, \tau_0 + \tau)$ for some $\tau < \tau_{nz}$.
- $A_\infty(t)$ is odd around $t = \tau_0$, i.e. $A_\infty(\tau_0 + \xi) = -A_\infty(\tau_0 - \xi)$ for $\xi \geq 0$
- $A_\infty(t)$ is continuous. $\triangle$

The properties outlined in Theorem 1 will be key to the synchronization mechanism we describe. The specific value of $\bar{\sigma}^2$ will be determined by our choice of the pulse-connection function. Before we prove Theorem 1 in Section III-C.2 we develop and motivate a few important related lemmas.

1) Polarity and Continuity of $A_\infty(t)$: At time $t = \tau_1 \neq \tau_0$, we have that

$$A_N(\tau_1) \;=\; \sum_{i=1}^{N} \frac{A_{max} K_i}{N} p(\tau_1 - \tau_0 - T_i) \;=\; \sum_{i=1}^{N} \frac{1}{N} \bar{M}_i(\tau_1),$$

where $\bar{M}_i(\tau_1) \overset{\Delta}{=} A_{max} K_i p(\tau_1 - \tau_0 - T_i)$. We have the mean of $\bar{M}_i(\tau_1)$ being

$$E(\bar{M}_i(\tau_1)) = A_{max} E(K_i) \int p(\tau_1 - \tau_0 - \psi) f_{T_i}(\psi) d\psi, \tag{11}$$

where $f_{T_i}(\psi)$ is the Gaussian pdf

$$f_{T_i}(\psi) = \frac{1}{\frac{\bar{\sigma}}{\alpha_i}\sqrt{2\pi}} \exp\left\{ -\frac{(\psi)^2}{2\frac{\bar{\sigma}^2}{\alpha_i^2}} \right\}.$$

It is clear that the $\bar{M}_i(\tau_1)$'s, for different i's, do not have the same mean and do not have the same variance since the two quantities depend on the α_i value. Since the α_i's are characterized by $f_\alpha(s)$ (defined in Section III-A), we write the Gaussian distribution for T as

$$f_T(\psi, s) = \frac{1}{\frac{\bar{\sigma}}{s}\sqrt{2\pi}} \exp\left\{ -\frac{(\psi)^2}{2\frac{\bar{\sigma}^2}{s^2}} \right\}.$$

and $\bar{M}_i(\tau_1)$ is in fact a function of s as well, denoted $\bar{M}_i(\tau_1, s)$. Using $f_T(\psi, s)$ and $\bar{M}_i(\tau_1, s)$, the notation makes it clear that we can average over the α_i's that are characterized by $f_\alpha(s)$. We use the results of Lemmas 1 and 2 to prove the polarity result for $A_\infty(t)$ in Section III-C.2.

Lemma 1: Given the sequence of independent random variables $\bar{M}_i(\tau_1)$ with $\tau_1 < \tau_0$, $E(\bar{M}_i(\tau_1)) = \mu_i$, and $\mathrm{Var}(\bar{M}_i(\tau_1)) = \sigma_i^2$. Then, for all i,

$$\gamma_2 > \mu_i > \gamma_1 > 0 \tag{12}$$

$$\sigma_i^2 < \gamma_3 < \infty, \tag{13}$$

for some constants γ_1, γ_2, and γ_3 and

$$\lim_{N \to \infty} \frac{1}{N} \sum_{i=1}^{N} \bar{M}_i(\tau_1) = \eta(\tau_1) > 0$$

almost surely, where

$$\begin{aligned}
\eta(\tau_1) &= \int_{\alpha_{low}}^{\alpha_{up}} E(\bar{M}_i(\tau_1, s)) f_\alpha(s) ds \\
&= A_{max} E(K_i) \int_{\alpha_{low}}^{\alpha_{up}} \int_{-\infty}^{\infty} p(\tau_1 - \tau_0 - \psi) f_T(\psi, s) d\psi f_\alpha(s) ds. \qquad \triangle
\end{aligned}$$

Lemma 2: Given the sequence of independent random variables $\bar{M}_i(\tau_1)$ with $\tau_1 > \tau_0$, $E(\bar{M}_i(\tau_1)) = \mu_i$, and $\text{Var}(\bar{M}_i(\tau_1)) = \sigma_i^2$. Then, for all i,

$$\gamma_2 < \mu_i < \gamma_1 < 0 \tag{14}$$

$$\sigma_i^2 < \gamma_3 < \infty, \tag{15}$$

for some constants γ_1, γ_2, and γ_3 and

$$\lim_{N \to \infty} \frac{1}{N} \sum_{i=1}^{N} \bar{M}_i(\tau_1) = \eta(\tau_1) < 0$$

almost surely, where

$$\eta(\tau_1) = \int_{\alpha_{low}}^{\alpha_{up}} E(\bar{M}_i(\tau_1, s)) f_\alpha(s) ds. \qquad \triangle$$

The results of Lemma 1 and Lemma 2 are intuitive since given that $p(t)$ is odd and the Gaussian noise distribution is symmetric, it makes sense for $A_\infty(t)$ to have properties similar to an odd waveform. Since the proofs of the two lemmas are very similar, we only prove Lemma 1. The proof can be found in the appendix.

Knowing only the polarity of $A_\infty(t)$ is not entirely satisfying since we would also expect that the limiting waveform be continuous. The proof of Lemma 3 is once again left for the appendix.

Lemma 3: Using $p(t)$ in (8),

$$A_\infty(t) = \lim_{N \to \infty} \frac{1}{N} \sum_{i=1}^{N} A_{max} K_i p(t - \tau_0 - T_i) = \lim_{N \to \infty} \frac{1}{N} \sum_{i=1}^{N} \bar{M}_i(t) = \eta(t)$$

is a continuous function of t, where

$$\begin{aligned}
\eta(t) &= \int_{\alpha_{low}}^{\alpha_{up}} E(\bar{M}_i(t, s)) f_\alpha(s) ds \\
&= A_{max} E(K_i) \int_{\alpha_{low}}^{\alpha_{up}} \int_{-\infty}^{\infty} p(t - \tau_0 - \psi) f_T(\psi, s) d\psi f_\alpha(s) ds. \qquad \triangle
\end{aligned}$$

2) Proof of Theorem 1: We can proceed in a straightforward manner to show that $A_\infty(\tau_0) = 0$. For $t = \tau_o$,

$$A_N(\tau_0) = \sum_{i=1}^{N} \frac{A_{max}K_i}{N} p(\tau_0 - \tau_0 - T_i) = \frac{1}{N}\sum_{i=1}^{N} A_{max}K_i p(-T_i) = \frac{1}{N}\sum_{i=1}^{N} M_i,$$

where $M_i \triangleq -A_{max}K_i p(T_i)$.

Since our goal is to apply some form of the strong law of large numbers, we first examine the mean of M_i. We have that $E(M_i) = -A_{max}E(K_i)E(p(T_i))$. Furthermore,

$$E(p(T_i)) = \int_{-\infty}^{\infty} p(\psi)f_{T_i}(\psi)d\psi = 0,$$

since $p(\psi)$ is odd and $f_{T_i}(\psi)$ is even because it is zero-mean Gaussian. Thus, $E(M_i) = 0$.

We next consider the variance of M_i:

$$\begin{aligned}
\mathrm{Var}(M_i) &= E(M_i^2) - E^2(M_i) = A_{max}^2 E(K_i^2 p^2(T_i)) \\
&= A_{max}^2 E(K_i^2)E(p^2(T_i)) < A_{max}^2 < \infty,
\end{aligned}$$

where we have used the fact that $E(K_i^2) \le 1$ and $|p(t)| \le 1$.

From the preceding discussion we see that the M_i's are a sequence of zero mean, finite (but possibly different) variance random variables. From Stark and Woods [38], we know that if $\sum_{i=1}^{\infty} \mathrm{Var}(M_i)/i^2 < \infty$, then we have strong convergence of the M_i's:

$$\frac{1}{N}\sum_{i=1}^{N} M_i \to E(M_i),$$

with probability-1 as $N \to \infty$. But it is easy to see that

$$\sum_{i=1}^{\infty} \frac{\mathrm{Var}(M_i)}{i^2} < \sum_{i=1}^{\infty} \frac{A_{max}^2}{i^2} = A_{max}^2 \frac{\pi^2}{6} < \infty,$$

so the condition is satisfied. As a result,

$$A_N(\tau_0) = \frac{1}{N}\sum_{i=1}^{N} M_i \to 0,$$

as $N \to \infty$.

We have that $A_\infty(t)$ is continuous from Lemma 3. Thus, next we need to show that $A_\infty(t) > 0$ for $t \in (\tau_0 - \tau, \tau_0)$, and $A_\infty(t) < 0$ for $t \in (\tau_0, \tau_0 + \tau)$ for some $\tau < \tau_{nz}$. We show the case for $t = \tau_1 \in (\tau_0 - \tau, \tau_0)$ by simply applying Lemma 1. Since Lemma 1 holds for all $\tau_1 < \tau_0$, there clearly exists a τ such $A_\infty(t) > 0$ for $t \in (\tau_0 - \tau, \tau_0)$. The case for $t \in (\tau_0, \tau_0 + \tau)$ comes similarly from Lemma 2.

Lastly, it remains to be shown that $A_\infty(t)$ is odd around $t = \tau_0$. This, however, is evident from the form of $\eta(t)$. Since $f_T(\psi, s)$ is even in ψ about 0 and $p(\psi)$ is odd about 0, it is clear that $\int_\infty^\infty p(t - \tau_0 - \psi) f_T(\psi, s) d\psi$ as a function of t is odd about τ_0. Thus, $\eta(t)$ is odd around τ_0. This then completes the proof for Theorem 1. $\triangle$

IV. ASYMPTOTIC TIME SYNCHRONIZATION

A. *The Use of Estimators in Time Synchronization*

In this work we want to show that as we let $N \to \infty$ then we can recover deterministic parameters that allow for time synchronization. Such a result would provide rigorous theoretical support for a new trade-off between network density and synchronization performance. To simplify the study, we focus on the steady-state time synchronization properties of asymptotically dense networks. In particular, we develop a cooperative technique that constructs a sequence of equispaced zero-crossings seen by all nodes which allows the network to maintain time synchronization indefinitely given that the nodes start with a collection of equispaced zero-crossings. Starting with a few equispaced zero-crossings allows us to avoid the complexities of starting up the synchronization process but still allows us to show that spatial averaging can be used to average out timing errors. If we are able to maintain indefinitely a sequence of equispaced zero-crossing using cooperative time synchronization, then it means that spatial averaging can average out all uncertainties in the system as we let node density grow unbounded. This recovery of deterministic parameters is our desired result. Here, we overview the estimators needed for cooperative time synchronization.

Let $t_{n,i}^{c_k}$ be the time, with respect to clock c_k, that the ith node sees its nth pulse. In dealing with the steady-state properties, we start by assuming that each node i in the network has observed a sequence of m pulse arrival times, $t_{n-1,i}^{c_i}, \ldots, t_{n-m,i}^{c_i}$, that occur at integer values of t, m is an integer. Recall that $t_{n-1,i}^{c_i}, \ldots, t_{n-m,i}^{c_i}$ is defined as a set of m pulse arrival times in the time scale of c_i. Therefore, even though $t_{n-1,i}^{c_i}, \ldots, t_{n-m,i}^{c_i}$ occur at integer values of t (the time scale of c_1), these values are not necessarily integers since they are in the time scale of c_i. Note also that in our model the pulse arrival time is a zero-crossing location. Using these m pulse arrival times, each node i has two distinct, yet closely related tasks. The first task is time synchronization. To achieve time synchronization, node i wants to use these m pulse arrival times to make an estimate of when the next zero-crossing will occur. If it can estimate this next zero-crossing time, then it can effectively estimate the next integer value of t. This estimator can then be extended to estimate arbitrary times in the future which gives node i the ability to synchronize to node 1. The second task is that node i needs to transmit a pulse so that the

sum of all pulses from the N nodes in the network will create an aggregate waveform that, in the limit as $N \to \infty$, will give a zero-crossing at the next integer value of t. This second task is very significant because if the aggregate waveform gives the exact location of the next integer value of t, then each node i in the network can use this new zero-crossing along with $t_{n-1,i}^{c_i}, \ldots, t_{n-m+1,i}^{c_i}$ to form a set of m zero-crossing locations. This new set can then be used to predict the next zero-crossing location as well as node i's next pulse transmission time. Recall that determining the pulse transmission time is the job of the pulse-connection function $X_{n,i}^{c_i}$. With such a setup, synchronization would be maintained indefinitely. The zero-crossings that always occur at integer values of t would provide node i a sequence of synchronization events and also illustrate how cooperation is averaging out all random errors.

The waveform properties detailed in Theorem 1 play a central role in accomplishing the nodes' task of cooperatively generating an aggregate waveform with a zero-crossing at the next integer value of t. From (10), if the arrival time of any pulse at a node j is a random variable of the form $\tau_0 + T_i$, where τ_0 is the next integer value of t and T_i is zero-mean Gaussian (or in general any symmetric random variable with zero-mean and finite variance), then Theorem 1 tells us that the aggregate waveform will make a zero-crossing at the next integer value of t. This idea is illustrated in Fig. 6.
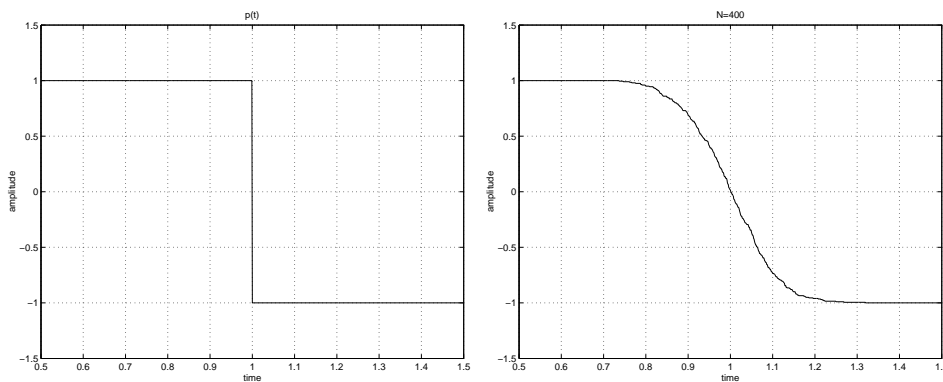

Fig. 6. Theorem 1 is key in explaining the intuition first illustrated in Fig. 1. The pulse $p(t)$ is shown on the left figure, with $\tau_0 = 1$ and $A_{max} = 1$. On the right we have a realization of $A_N(t)$ ($N = 400$), and we assume that $K_{j,i} = 1$ (no path loss) and $T_i \sim \mathcal{N}(0, 0.01)$ for all i. As expected from Theorem 1, we notice that the zero-crossing of the simulated waveform is almost exactly at $t = 1$.

Thus, for achieving time synchronization in an asymptotically dense network we need to address two issues. First, we need to develop an estimator for the next integer value of t given a sequence of m pulse arrival times that occur at integer values of t. We will call this the *time synchronization estimator* and let us write $V_{n,i}^{c_i}$ as the time synchronization estimator that determines the time, in the time scale of c_i, when

node i predicts it will see its nth zero-crossing. Two, we need to develop the pulse-connection function $X_{n,i}^{c_i}$ such that node i's transmitted pulse will arrive at a node j with the random properties described in Theorem 1.

B. Time Synchronization Estimator Performance Measure

Here we establish the conditions for estimating the next pulse arrival time, or equivalently the next integer value of t, given m pulse arrival times. These conditions apply most directly to the time synchronization estimator $V_{n,i}^{c_i}$ since we want to synchronize in some desired manner. The problem of synchronization is the challenge of having the ith node accurately and precisely predict when the next integer value of t will occur. In our setup, the reception of a pulse by node i tells it of such an event.

Let us explicitly model the time at an integer value of t in terms of the clock of node i. Assume τ_0 is an integer value of t and at this time, node i will observe its nth pulse. Thus, from (1) we have that

$$t_{n,i}^{c_i} = \alpha_i(\tau_0 - \bar{\Delta}_i) + \Psi_i(\tau_0). \tag{16}$$

The equation makes use of the clock model of node i (1) to tell us the time at clock c_i when node 1 is at τ_0, where τ_0 is an integer in the time scale of c_1. We are also starting with the assumption that the zero-crossing that occurs at an integer value of t is observed by node i at this time.

From (16) we see that the pulse receive time at node i, $t_{n,i}^{c_i}$, is a Gaussian random variable whose mean is parameterized by the unknown vector $\vartheta = [\alpha_i, \tau_0, \bar{\Delta}_i]$. Thus, to achieve synchronization node i will try to estimate the random variable $t_{n,i}^{c_i}$ using a series of m pulse receive times as observations (recall that m is known). Note that the observations are also random variables with distributions parameterized by ϑ. We want the time synchronization estimator of node i to make an estimate of $t_{n,i}^{c_i}$, denoted $\hat{t}_{n,i}^{c_i}(t_{n-1,i}^{c_i}, t_{n-2,i}^{c_i}, \ldots, t_{n-m,i}^{c_i})$ which is a function of past observations $t_{n-1,i}^{c_i}, t_{n-2,i}^{c_i}, \ldots, t_{n-m,i}^{c_i}$, that meets the following criteria:

$$E_\vartheta\left[\hat{t}_{n,i}^{c_i}(t_{n-1,i}^{c_i}, t_{n-2,i}^{c_i}, \ldots, t_{n-m,i}^{c_i})\right] = E_\vartheta(t_{n,i}^{c_i}) \tag{17}$$

$$\mathrm{argmin}_{\hat{t}_{n,i}^{c_i}} E_\vartheta\left[(\hat{t}_{n,i}^{c_i}(t_{n-1,i}^{c_i}, t_{n-2,i}^{c_i}, \ldots, t_{n-m,i}^{c_i}) - t_{n,i}^{c_i})^2\right] \tag{18}$$

for all ϑ. The subscript ϑ means that the expectation is taken over the distributions involved given any possible ϑ. The first condition comes from the fact that given a finite m, it is reasonable to want the expected value of the estimate to be the expected value of the random variable being estimated for all ϑ. As in the justification for unbiased estimators, this condition eliminates unreasonable estimators so that the chosen estimator will perform well, on average, for all values of ϑ [33]. The second condition is

the result of seeking to minimize the mean squared error between the estimate and the random variable being estimated for all ϑ.

C. Time Synchronization Estimator

For the time synchronization estimator, node i will seek to estimate $t_{n,i}^{c_i}$ given $t_{n-1,i}^{c_i}, \ldots, t_{n-m,i}^{c_i}$. From (16), we see that $\mathbf{T} = [t_{n-m,i}^{c_i}, \ldots, t_{n-1,i}^{c_i}]^T$ is a jointly Gaussian random vector parameterized by ϑ. Recall that we assume $\Psi_i(t)$ is a zero mean Gaussian process with independent and identically distributed samples $\Psi_i(t) \sim \mathcal{N}(0, \sigma^2)$, for any t. Also, since we're assuming that the zero-crossings at node i occur at consecutive integer values of t, the random variable $t_{n-m,i}^{c_i}$ is Gaussian with $t_{n-m,i}^{c_i} \sim \mathcal{N}(\alpha_i(\tau_0 - m - \bar{\Delta}_i), \sigma^2)$ for some $\vartheta = [\alpha_i, \tau_0 - m, \bar{\Delta}_i]$. We also notice that

$$E_\vartheta(t_{n-m+1,i}^{c_i}) = \alpha_i(\tau_0 - m + 1 - \bar{\Delta}_i) = \alpha_i(\tau_0 - m - \bar{\Delta}_i) + \alpha_i.$$

Since each noise sample is independent, we see that the distribution of $\mathbf{T}$ parameterized by ϑ can be written as $\mathbf{T} \sim \mathcal{N}(\mathbf{M}, \Sigma)$ where

$$\mathbf{M} = \begin{bmatrix} \alpha_i(\tau_0 - m - \bar{\Delta}_i) \\ \alpha_i(\tau_0 - m - \bar{\Delta}_i) + \alpha_i \\ \alpha_i(\tau_0 - m - \bar{\Delta}_i) + 2\alpha_i \\ \vdots \\ \alpha_i(\tau_0 - m - \bar{\Delta}_i) + (m-1)\alpha_i \end{bmatrix}$$

and $\Sigma = \sigma^2 \mathbf{I}$.

As a result, for any m consecutive observations, we can simplify notation by using the model

$$\mathbf{Y} = \mathbf{H}\theta + \mathbf{W}, \tag{19}$$

where $\mathbf{Y} = \begin{bmatrix} Y_1 & Y_2 \ldots Y_m \end{bmatrix}^T = \begin{bmatrix} t_{n-m,i}^{c_i} & t_{n-m+1,i}^{c_i} \ldots t_{n-1,i}^{c_i} \end{bmatrix}^T$ and

$$\theta = \begin{bmatrix} \theta_1 \\ \theta_2 \end{bmatrix} = \begin{bmatrix} \alpha_i(\tau_0 - m - \bar{\Delta}_i) \\ \alpha_i \end{bmatrix}$$

with

$$\mathbf{H} = \begin{bmatrix} 1 & 1 & 1 & \ldots & 1 \\ 0 & 1 & 2 & \ldots & m-1 \end{bmatrix}^T$$

and $\mathbf{W} = [W_1 \ldots W_m]^T$. Since $\Psi_i(t)$ is a Gaussian noise process, $\mathbf{W} \sim \mathcal{N}(0, \Sigma)$ with $\Sigma = \sigma^2 \mathbf{I}$.

Using the simplified notation in (19), we want to estimate Y_{m+1}, where Y_{m+1} is jointly distributed with $\mathbf{Y}$ as

$$\begin{bmatrix} \mathbf{Y} \\ Y_{m+1} \end{bmatrix} \sim \mathcal{N}(\begin{bmatrix} \mathbf{M} \\ \theta_1 + m\theta_2 \end{bmatrix}, \begin{bmatrix} \Sigma & 0 \\ 0 & \sigma^2 \end{bmatrix}).$$

Using this notation, we can rewrite the synchronization criteria as:

$$E_\theta\big[\hat{Y}_{m+1}(Y_1, Y_2, \ldots, Y_m)\big] = E_\theta(Y_{m+1}) \tag{20}$$

$$\operatorname{argmin}_{\hat{Y}_{m+1}} E_\theta\big[(\hat{Y}_{m+1}(Y_1, Y_2, \ldots, Y_m) - Y_{m+1})^2\big], \tag{21}$$

where $\hat{Y}_{m+1}$ is the estimator for Y_{m+1}.

Condition (20) implies that our estimate must be unbiased. Condition (21) is equivalent to

$$\operatorname{argmin}_{\hat{Y}_{m+1}} E_\theta\big[(\hat{Y}_{m+1}(Y_1, Y_2, \ldots, Y_m) - (\theta_1 + m\theta_2))^2\big].$$

To see this equivalence, note that

$$\begin{aligned}
& E_\theta\big[(\hat{Y}_{m+1}(Y_1, Y_2, \ldots, Y_m) - Y_{m+1})^2\big] \\
&= E_\theta\big[(\hat{Y}_{m+1}(Y_1, Y_2, \ldots, Y_m) - (\theta_1 + m\theta_2) - W_{m+1})^2\big] \\
&= E_\theta\big[(\hat{Y}_{m+1}(Y_1, Y_2, \ldots, Y_m) - (\theta_1 + m\theta_2))^2\big] + E\big[W_{m+1}^2\big], \tag{22}
\end{aligned}$$

where the last inequality follows from the independence of W_{m+1} from all other noise samples. Since the distribution of of W_{m+1} is independent of θ,

$$\begin{aligned}
& \operatorname{argmin}_{\hat{Y}_{m+1}} E_\theta\big[(\hat{Y}_{m+1}(Y_1, Y_2, \ldots, Y_m) - Y_{m+1})^2\big] \\
&= \operatorname{argmin}_{\hat{Y}_{m+1}} E_\theta\big[(\hat{Y}_{m+1}(Y_1, Y_2, \ldots, Y_m) - (\theta_1 + m\theta_2))^2\big].
\end{aligned}$$

With these two conditions, from [33] we see that the desired estimate for Y_{m+1} will be the uniformly minimum variance unbiased (UMVU) estimator for $E_\theta(Y_{m+1}) = \theta_1 + m\theta_2$.

Using the above linear model, from [23] we know the maximum likelihood (ML) estimate of θ, $\hat{\theta}_{ML}$, is given by

$$\hat{\theta}_{ML} = (\mathbf{H}^T \Sigma^{-1} \mathbf{H})^{-1} \mathbf{H}^T \Sigma^{-1} \mathbf{Y} = (\mathbf{H}^T \mathbf{H})^{-1} \mathbf{H}^T \mathbf{Y}. \tag{23}$$

This estimate achieves the Cramer Rao lower bound, hence is efficient. The Fisher information matrix is $I(\theta) = \frac{\mathbf{H}^T \mathbf{H}}{\sigma^2}$ and $\hat{\theta}_{ML} \sim \mathcal{N}(\theta, \sigma^2(\mathbf{H}^T \mathbf{H})^{-1})$. This means that $\hat{\theta}_{ML}$ is UMVU.

Again from [23], the invariance of the ML estimate tells us that the ML estimate for $\phi = g(\theta) = \theta_1 + m\theta_2$ is $\hat{\phi}_{ML} = \hat{\theta}_{1ML} + m\hat{\theta}_{2ML}$. First, it is clear that $\hat{\phi}_{ML} = \mathbf{C}\hat{\theta}_{ML}$, where $\mathbf{C} = [1 \quad m]$. As a

result, we first see that $E_\theta(\hat{\phi}_{ML}) = \mathbf{C}E_\theta(\hat{\theta}_{ML}) = \theta_1 + m\theta_2$ so $\hat{\phi}_{ML}$ is unbiased. Next, to see that $\hat{\phi}_{ML}$ is also minimum variance we compare its variance to the lower bound.

$$\text{Var}_\theta(\hat{\phi}_{ML}) = \mathbf{C}\sigma^2(\mathbf{H}^T\mathbf{H})^{-1}\mathbf{C}^T = \frac{2\sigma^2(2m+1)}{m(m-1)}.$$

The extension of the Cramer Rao lower bound in [23] to a function of parameters tells us that

$$E_\theta(\|\hat{g} - g(\theta)\|^2) \geq \mathbf{G}(\theta)\mathbf{I}^{-1}(\theta)\mathbf{G}^T(\theta)$$

with $\mathbf{G}(\theta) = (\nabla_\theta g(\theta))^T$. In this case, $\mathbf{G}(\theta) = \begin{bmatrix} 1 & m \end{bmatrix}$ so the lower bound to the mean squared error is

$$\mathbf{G}(\theta)\mathbf{I}^{-1}(\theta)\mathbf{G}^T(\theta) = \frac{2\sigma^2(2m+1)}{m(m-1)}.$$

As a result, we see that $\hat{\phi}_{ML}$ is UMVU. Since $\hat{\phi}_{ML}$ is the desired estimate of where the next pulse arrival time will be, it is the time synchronization estimator. Thus,

$$V_{n,i}^{c_i}(\mathbf{Y}) = \mathbf{C}(\mathbf{H}^T\mathbf{H})^{-1}\mathbf{H}^T\mathbf{Y}. \tag{24}$$

Note that

$$V_{n,i}^{c_i}(\mathbf{Y}) = \hat{\phi}_{ML} \sim \mathcal{N}\left(\phi, \frac{2\sigma^2(2m+1)}{m(m-1)}\right). \tag{25}$$

has a variance that goes to zero as $m \to \infty$.

D. Time Synchronization with No Propagation Delay

We now need to develop the pulse-connection function so that the conditions for T_i in Theorem 1 are satisfied. Recall we are developing the synchronization technique under the assumption of no propagation delay, i.e. $\delta(d) = 0$. Given a sequence of m pulse arrival times, the time synchronization estimator $V_{n,i}^{c_i}$ given in (24) gives each node the ability to predict the next integer value of t. What remains to be considered is the second part of the synchronization process: developing a pulse-connection function $X_{n,i}^{c_i}$ such that the aggregate waveform seen by a node j will have the properties described in Theorem 1.

Let us first consider the distribution of $V_{n,i}^{c_i}$. From (25), we have that

$$V_{n,i}^{c_i}(\mathbf{Y}) \sim \mathcal{N}\left(\alpha_i(\tau_0 - m - \bar{\Delta}_i) + m\alpha_i, \frac{2\sigma^2(2m+1)}{m(m-1)}\right).$$

Using (1), we can translate $V_{n,i}^{c_i}(\mathbf{Y})$ into the time scale of c_1 as

$$V_{n,i}^{c_i}(\mathbf{Y}) = \alpha_i(V_{n,i}^{c_1}(\mathbf{Y}) - \bar{\Delta}_i) + \Psi_i$$

which gives

$$V_{n,i}^{c_1}(\mathbf{Y}) = \frac{(V_{n,i}^{c_i}(\mathbf{Y}) - \Psi_i)}{\alpha_i} + \bar{\Delta}_i.$$

This means that

$$V_{n,i}^{c_1}(\mathbf{Y}) \sim \mathcal{N}\left(\tau_0, \frac{\sigma^2}{\alpha_i^2}\left(1 + \frac{2(2m+1)}{m(m-1)}\right)\right). \tag{26}$$

Under our assumption of $\delta(d) = 0$, any transmission by node i will be instantaneously seen by any node j. As a result, the random variable $V_{n,i}^{c_1}(\mathbf{Y})$ will be seen as the pulse arrival time at node j, in the time scale of c_1.

Due to the assumption of no propagation delay, defining $X_{n,i}^{c_1}(\mathbf{Y}) \triangleq V_{n,i}^{c_1}(\mathbf{Y})$ will give us the desired properties in the aggregate waveform. To see this, let us compare the distribution of $X_{n,i}^{c_1}(\mathbf{Y})$ to the assumptions of Theorem 1. Since τ_0 is the ideal crossing time in the time scale of c_1, we have

$$X_{n,i}^{c_1}(\mathbf{Y}) = \tau_0 + T_i.$$

Therefore, we see that

$$\text{Var}(T_i) = \frac{\sigma^2}{\alpha_i^2}\left(1 + \frac{2(2m+1)}{m(m-1)}\right) = \frac{\bar{\sigma}^2}{\alpha_i^2}, \tag{27}$$

where $\bar{\sigma}^2$ from Theorem 1 is

$$\bar{\sigma}^2 = \sigma^2\left(1 + \frac{2(2m+1)}{m(m-1)}\right).$$

We have shown that using the pulse connection function $X_{n,i}^{c_1}(\mathbf{Y}) \triangleq V_{n,i}^{c_1}(\mathbf{Y})$ satisfies the conditions of Theorem 1. Thus, all the results of the theorem apply.

As a result, we have established a time synchronization estimator $V_{n,i}^{c_1}(\mathbf{Y})$ and a pulse-connection function $X_{n,i}^{c_1}(\mathbf{Y})$. In the case of $\delta(d) = 0$, we have that $X_{n,i}^{c_1}(\mathbf{Y}) \triangleq V_{n,i}^{c_1}(\mathbf{Y})$, or in the time scale of c_i, $X_{n,i}^{c_i}(\mathbf{Y}) \triangleq V_{n,i}^{c_i}(\mathbf{Y})$. When each node in the network uses the pulse-connection function $X_{n,i}^{c_i}(\mathbf{Y})$ we have a resulting aggregate waveform that has a zero-crossing at the next integer value of t as $N \to \infty$. This fact follows from applying Theorem 1. Thus, we have an asymptotic steady-state time synchronization method that can maintain a sequence of equispaced zero-crossings occurring at integer values of t. An interesting feature of this synchronization technique is that no node needs to know any information about its location or its surrounding neighbors.

1) Cooperation without Simultaneous Transmission and Reception: Before ending this section, let us comment on the assumption of simultaneous transmission and reception. One way to relax this assumption is to divide the network into two disjoint sets of nodes, say the odd numbered nodes and the even numbered nodes, where each set is still uniformly distributed over the area. Then, the odd nodes and the even nodes will take turns transmitting and receiving. For example, the odd numbered nodes can transmit pulses at odd values of t and the even numbered nodes will listen. The even numbered nodes will then transmit pulses at the even values of t and the odd numbered nodes will listen. With such a scheme, nodes do

not transmit and receive pulses simultaneously, but can still take advantage of spatial averaging. The odd numbered nodes will see an aggregate waveform generated by a subset of the even numbered nodes and the even numbered nodes will receive a waveform cooperatively generated by the odd numbered nodes. Let us take a more detailed look at this scheme.
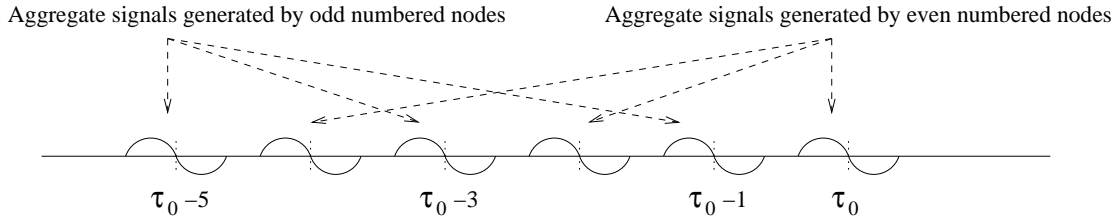

Fig. 7. In the above figure, we assume τ_0 is an even integer value of t and $m = 3$. Therefore, each even numbered node will turn on its receiver to receive the aggregate signal arriving at times $\tau_0 - 5$, $\tau_0 - 3$, and $\tau_0 - 1$. Using these three received times, it can then estimate the time of τ_0. Thus, the aggregate signal occurring at τ_0 is cooperatively generated by the even numbered nodes and is received by the odd numbered nodes.

In Fig. 7 we assume that τ_0 is an even integer value of t and use $m = 3$. Each even numbered node will use the aggregate signals occurring at $\tau_0 - 5$, $\tau_0 - 3$, and $\tau_0 - 1$ to estimate τ_0 and cooperatively the even nodes will generate the aggregate signal at τ_0. The odd numbered nodes will then use the aggregate signals occurring at $\tau_0 - 4$, $\tau_0 - 2$, and τ_0 to generate the aggregate signal at $\tau_0 + 1$. Therefore, the odd and even numbered nodes can take turns transmitting and receiving signals and nodes never need to simultaneously transmit and receive.

Of course, such a setup would require a modification of the estimators used by the nodes. Nodes will receive a vector of m observations $\mathbf{Y}$ with $\mathbf{Y}[l+1] = \alpha_i(\tau_0 + 1 - 2(m-l) - \bar{\Delta}_i) + \Psi_i$ for $l = 0, 1, \ldots, m-1$. With such a mechanism, the $\mathbf{H}$ matrix in equation (19) would change to

$$\mathbf{H} = \begin{bmatrix} 1 & 1 & 1 & \ldots & 1 \\ 0 & 2 & 4 & \ldots & 2(m-1) \end{bmatrix}^T$$

and θ becomes

$$\theta = \begin{bmatrix} \theta_1 \\ \theta_2 \end{bmatrix} = \begin{bmatrix} \alpha_i(\tau_0 + 1 - 2m - \bar{\Delta}_i) \\ \alpha_i \end{bmatrix}.$$

To estimate the location τ_0 in the time scale of c_i, we can proceed as in Section IV-C:

$$\hat{\theta}_{ML} = (\mathbf{H}^T \Sigma^{-1} \mathbf{H})^{-1} \mathbf{H}^T \Sigma^{-1} \mathbf{Y} = (\mathbf{H}^T \mathbf{H})^{-1} \mathbf{H}^T Y$$

will be distributed $\hat{\theta}_{ML} \sim \mathcal{N}(\theta, \sigma^2(\mathbf{H}^T\mathbf{H})^{-1})$ and $\hat{\theta}_{ML}$ is UMVU. This leads to the UMVU estimate $\hat{\phi}_{ML} = \mathbf{C}\hat{\theta}_{ML}$, where $\mathbf{C} = [1 \quad 2m - 1]$, and $E(\hat{\phi}_{ML}) = \mathbf{C}E(\hat{\theta}_{ML}) = \theta_1 + (2m - 1)\theta_2$. In this case, the variance of $\hat{\phi}_{ML}$ will be $\text{Var}_\theta(\hat{\phi}_{ML}) = \mathbf{C}\sigma^2(\mathbf{H}^T\mathbf{H})^{-1}\mathbf{C}^T$, and thus we have that

$$V_{n,i}^{c_i}(\mathbf{Y}) = \hat{\phi}_{ML} \sim \mathcal{N}\left(\alpha_i(\tau_0 + 1 - 2m - \bar{\Delta}_i) + (2m - 1)\alpha_i, \frac{\sigma^2(2m + 1)(2m - 1)}{m(m - 1)(m + 1)}\right).$$

Converted to the time scale of c_1 we have

$$V_{n,i}^{c_1}(\mathbf{Y}) \sim \mathcal{N}\left(\tau_0, \frac{\sigma^2}{\alpha_i^2}\left(1 + \frac{(2m + 1)(2m - 1)}{m(m - 1)(m + 1)}\right)\right). \tag{28}$$

Comparing equations (26) and (28), we see that they have the same form. As a result, we can again set $X_{n,i}^{c_i}(\mathbf{Y}) \triangleq V_{n,i}^{c_i}(\mathbf{Y})$ and achieve cooperative time synchronization.

V. TIME SYNCHRONIZATION WITH PROPAGATION DELAY

We now extend the ideas of cooperative time synchronization to the situation where signals suffer not only from pathloss but also propagation delay. It turns out that the effect of propagation delay can also be addressed using the concept we have been using throughout this paper — averaging out errors using the large number of nodes in the network.

In this section, we use the pathloss and propagation delay model detailed in Section II-C. We introduce a time delay function $\delta(d)$. For generality, we explicitly model a multi-hop network where we have a $K(d)$ function that is zero for d greater than some distance R, i.e. $K(d) = 0$ for $d > R$. Such a model implies that the aggregate signal seen at any node j is influenced only by the set of nodes inside a circle of radius R centered at node j. With this we can effectively divide the network into two disjoint sets, a set of *interior nodes* and a set of *boundary nodes*. An interior node j is defined to be a node whose distance from the nearest network boundary is greater than or equal to R. A boundary node is thus defined to be a node that is a distance less than R away from the nearest network boundary.

We make this distinction since the synchronization technique for each set of nodes is different. Please note that if a pathloss function where $K(d) = 0$ for $d > R$ is unreasonable, then we simply choose R to be infinite and consider all nodes in the network to be boundary nodes.

Using the propagation delay model, $D_{j,i}$ will obviously modify the general received aggregate waveform seen at any node j. In fact, equation (7) will now be written as

$$A_{j,N}^{c_1}(t) = \sum_{i=1}^{N} \frac{A_{max}K_{j,i}}{N} p(t - \tau_o - T_i - D_{j,i}). \tag{29}$$

For N large, this model will give an accurate characterization of the aggregate waveform seen at node j.

A. Conceptual Motivation

From equation (29), it is clear that the aggregate waveform will not have a zero-crossing at τ_0 for every node j because of the presence of the $D_{j,i}$ random variables. Therefore, to average out propagation delay, the idea we employ is to have each node introduce a *random* artificial time shift that counteracts the effect of the time delay random variable. More precisely, we want to introduce another random variable D_{fix} such that $D_{fix} + D_j$ will have zero mean and a symmetric distribution. At the same time, we assume each node knows $K(\cdot)$ and $\delta(\cdot)$ and will also introduce an artificial scaling factor $K_{fix} = K(\delta^{-1}(-D_{fix}))$ to simplify the analysis of the aggregate waveform. This means that instead of using the scaling factor $A_i = A_{max}/N$, each node i will scale its transmitted pulse by $A_i = A_{max}K_{fix}/N$. For the motivation in this section, let us assume that node j is an interior node.

To find the distribution of D_{fix}, we consider the following. D_j has density $f_{D_j}(x)$ and let $f_{D_{fix}}(x)$ be the density of D_{fix}. Since D_j and D_{fix} are independent, we know that the density of $D_T = D_{fix} + D_{j,i}$, $f_{D_T}(x)$, will be the convolution of $f_{D_j}(x)$ and $f_{D_{fix}}(x)$. Therefore, by the properties of the convolution function, if we set $f_{D_{fix}}(x) \triangleq f_{D_j}(-x)$, then we have that $f_{D_T}(x)$ is symmetric, i.e. $f_{D_T}(x) = f_{D_T}(-x)$. As well, since D_j has finite expectation, it is easy to see that $E(D_T) = 0$.

Given a sequence of m zero-crossings that we know to be occurring at integers of t, we can still use $V_{n,i}^{c_1}(\mathbf{Y})$ (from (24) in the time scale of node 1) as the time synchronization estimator. However, with propagation delay, the pulse-connection function will now be $X_{n,i}^{c_1}(\mathbf{Y}) = V_{n,i}^{c_1}(\mathbf{Y}) + D_{fix} = \tau_o + T_i + D_{fix}$. With D_{fix} and K_{fix} included, we can rewrite equation (29) as

$$A_{j,N}^{c_1}(t) = \sum_{i=1}^{N} \frac{A_{max}K_{fix}K_{j,i}}{N}p(t - \tau_o - T_i - D_{fix} - D_{j,i}). \tag{30}$$

It is important to see that since D_j has the same distribution for *all* interior nodes j, equation (30) holds for every node j that is an interior node. This means that for the network to cooperatively generate the waveform in (30) each transmit node i needs to have the following additional knowledge: (1) the distribution of D_{fix} whose density is $f_{D_{fix}}(x) \triangleq f_{D_j}(-x)$, where j is an interior node, and (2) the functions $K(\cdot)$ and $\delta(\cdot)$ to generate K_{fix}. With this knowledge, we can use equation (30) to study the aggregate waveform seen at any interior node j. In fact, we find that the aggregate waveform has limiting properties that are similar to those outlined in Theorem 1. These properties are described in Theorem 2.

Theorem 2: Let $p(t)$ be as defined in equation (8) and $T_i \sim \mathcal{N}(0, \frac{\bar{\sigma}^2}{\alpha_i^2})$ with $\bar{\sigma}^2 > 0$ a constant and $\frac{\bar{\sigma}^2}{\alpha_i^2} < B < \infty$ for all i, B a constant. $K_{j,i}$ and $D_{j,i}$ are defined as in Section II-C and D_{fix} with density $f_{D_{fix}}(x) \triangleq f_{D_j}(-x)$ is independent from $D_{j,i}$. $K_{fix} = K(\delta^{-1}(-D_{fix}))$ and let $D_{j,i}$, D_{fix},

and T_i be mutually independent for all i. Then, for any interior node j with $A_{j,N}^{c_1}(t)$ as defined in (30), $\lim_{N\to\infty} A_{j,N}^{c_1}(t) = A_{j,\infty}^{c_1}(t)$ has the properties

- $A_{j,\infty}^{c_1}(\tau_0) = 0$,
- $A_{j,\infty}^{c_1}(t)$ is odd around $t = \tau_0$, i.e. $A_{j,\infty}^{c_1}(\tau_0 + \xi) = -A_{j,\infty}^{c_1}(\tau_0 - \xi)$ for $\xi \geq 0$. $\qquad \triangle$

The proof of Theorem 2 is left for the appendix.

From the arguments so far, it seems that time synchronization with delay, at least for interior nodes, can be solved simply by modifying the pulse-connection function $X_{n,i}^{c_1}(\mathbf{Y})$ and changing the scaling factor to $A_i = A_{max}K_{fix}/N$. Theorem 2 tells us that the limiting aggregate waveform makes a zero-crossing at the next integer value of t and the waveform is odd. Thus, we can use this zero-crossing as a synchronization event and maintain synchronization in a manner identical to the technique used in the situation without propagation delay. This, however, unfortunately is not the case. In order to implement the above concept, we need to find the random variable, $D_{fix}^{c_i}$, in the time scale of c_i, that corresponds to D_{fix} such that

$$
\begin{aligned}
(V_{n,i}^{c_i}(\mathbf{Y}) + D_{fix}^{c_i})^{c_1} &= \frac{V_{n,i}^{c_i}(\mathbf{Y}) + D_{fix}^{c_i} - \Psi_i}{\alpha_i} + \bar{\Delta}_i \\
&= V_{n,i}^{c_1}(\mathbf{Y}) + \frac{D_{fix}^{c_i}}{\alpha_i} \\
&= V_{n,i}^{c_1}(\mathbf{Y}) + D_{fix}.
\end{aligned}
$$

This means that we need $D_{fix}^{c_i}/\alpha_i = D_{fix}$. However, each node i cannot find $D_{fix}^{c_i}$ that satisfies this since it does not know its α_i.

B. Time Synchronization of Interior Nodes

Since the ith node does not know its own value of α_i, to do time synchronization with propagation delay we can have each node estimate its α_i value. However, this estimate will not be perfect and we may no longer have the symmetric limiting aggregate waveform described by Theorem 2. This means that the center zero-crossing might occur some ϵ away from τ_0, τ_0 an integer value of t. However, steady-state time synchronization can be maintained if the network can use a sequence of m equispaced zero-crossings that occur at $t = \tau_0 - m + \epsilon, \tau_0 - m + 1 + \epsilon, \tau_0 - m + 2 + \epsilon, \ldots, \tau_0 - 1 + \epsilon$, where τ_0 is an integer value of t, to cooperatively generate a limiting aggregate waveform that has a zero-crossing at $\tau_0 + \epsilon$. In such a situation, the network will be able to construct a sequence of equispaced zero-crossings and maintain the occurrence of these zero-crossings indefinitely. The idea is the same as in the case without propagation delay, but the only difference here would be that the zero-crossings do not occur at integer values of t. Let us give a more formal description of this idea.

Using notation from Section IV-C, we start with the assumption that each interior node i has a sequence of m observations that has the form

$$\alpha_i(\tau_0 - m + l + \epsilon - \bar{\Delta}_i) + \Psi_i, \tag{31}$$

where $l = 0, 1, \ldots, m - 1$ and ϵ is known. To develop the time synchronization estimator $V_{n,i}^{c_i}(\mathbf{Y})$ and the pulse-connection function $X_{n,i}^{c_i}(\mathbf{Y})$, we consider the observations made by each node. If we assume that each node knows the value of ϵ, the vector of observations can be written as in (19)

$$\mathbf{Y} = \bar{\mathbf{H}}\theta + \mathbf{W},$$

where the matrix $\bar{\mathbf{H}}$ in this case is

$$\bar{\mathbf{H}} = \begin{bmatrix} 1 & 1 & 1 & \ldots & 1 \\ \epsilon & 1+\epsilon & 2+\epsilon & \ldots & m-1+\epsilon \end{bmatrix}^T.$$

Using this model, we can follow the development in Section IV-C to find the the time synchronization estimator

$$V_{n,i}^{c_i}(\mathbf{Y}, \epsilon) = \mathbf{C}(\bar{\mathbf{H}}^T\bar{\mathbf{H}})^{-1}\bar{\mathbf{H}}^T\mathbf{Y}, \tag{32}$$

where $\mathbf{C} = [1 \quad m]$. This estimator will give each node the ability to optimally estimate the next integer value of t. Note that the variance of the time synchronization estimator is

$$\text{Var}_\theta(V_{n,i}^{c_i}(\mathbf{Y}, \epsilon)) = \mathbf{C}\sigma^2(\bar{\mathbf{H}}^T\bar{\mathbf{H}})^{-1}\mathbf{C}^T = \sigma^2 \left(\frac{2(2m+1)}{m(m-1)} + \frac{12\epsilon(\epsilon - 1 - m)}{(m-1)m(m+1)} \right). \tag{33}$$

Using the time synchronization estimator, we can choose the pulse-connection function as

$$X_{n,i}^{c_i}(\mathbf{Y}) = V_{n,i}^{c_i}(\mathbf{Y}, \epsilon) + \hat{\alpha}_i D_{fix} = V_{n,i}^{c_i}(\mathbf{Y}, \epsilon) + D_{fix}^{c_i}, \tag{34}$$

where each time node i makes the estimate $V_{n,i}^{c_i}(\mathbf{Y}, \epsilon)$ it also estimates $\hat{\alpha}_i$ as

$$\hat{\alpha}_i = \bar{\mathbf{C}}(\bar{\mathbf{H}}^T\bar{\mathbf{H}})^{-1}\bar{\mathbf{H}}^T\mathbf{Y},$$

$\bar{\mathbf{C}} = [0 \quad 1]$. We find that $\hat{\alpha}_i \sim \mathcal{N}(\alpha_i, 12\sigma^2/((m-1)m(m+1)))$. Since, from Section V-A, we know we want $D_{fix}^{c_i}/\alpha_i = D_{fix}$, we have set $D_{fix}^{c_i} \triangleq \hat{\alpha}_i D_{fix}$. Notice that since $D_{fix}^{c_i}$ is simply a realization of D_{fix} multiplied by node i's estimate of α_i, node i can use the realization of D_{fix} and find $K_{fix} = K(\delta^{-1}(-D_{fix}))$.

With our choice of $X_{n,i}^{c_i}(\mathbf{Y})$ in (34), we see that

$$(V_{n,i}^{c_i}(\mathbf{Y}, \epsilon) + D_{fix}^{c_i})^{c_1} = V_{n,i}^{c_1}(\mathbf{Y}, \epsilon) + Z_i D_{fix} = \tau_0 + T_i + Z_i D_{fix},$$

where $Z_i \sim \mathcal{N}(1, 12\sigma^2/(\alpha_i^2(m-1)m(m+1)))$, and $\tau_0 + T_i = V_{n,i}^{c_1}(\mathbf{Y}, \epsilon)$. Because of the random factor Z_i, we see that $D_T = Z_i D_{fix} + D_{j,i}$ is no longer a symmetric distribution. As a result, the limiting aggregate waveform

$$A_{j,\infty}^{c_1}(t) = \lim_{N \to \infty} A_{j,N}^{c_1}(t) = \lim_{N \to \infty} \sum_{i=1}^{N} \frac{A_{max}K_{fix}K_{j,i}}{N} p(t - \tau_o - T_i - Z_i D_{fix} - D_{j,i}) \qquad (35)$$

may not have a zero-crossing at $t = \tau_0$.

Thus, if we can find an ϵ such that each node i using a set of observations of the form (31) allows the network to cooperatively generate the waveform in (35) that has its zero-crossing occurring at $t = \tau_0 + \epsilon$ (in the time scale of c_1), then we have steady-state time synchronization. This is because the network would be able to use a sequence of m observations to generate the next observation that gives the same information as any of the previous observations. Thus, by always taking the m most recent observations, the process can continue forever and maintain synchronization. Each node i would need to know distribution of D_{fix}, the value of ϵ, and the functions $K(\cdot)$ and $\delta(\cdot)$. Therefore, we find that steady-state time synchronization of the interior nodes is possible under certain conditions. As a note, no interior node needs to know any location information.

C. Time Synchronization of Boundary Nodes

Before we consider the synchronization of boundary nodes, we note that the key requirement for each boundary node i is to have a pulse-connection function given in equation (34). The reason that this must be the pulse-connection for every boundary node i is because the analysis for the interior nodes assumes that the aggregate waveform seen by any interior node j is created by pulse transmissions occurring at a time determined by (34). Since the aggregate waveform seen by some interior nodes are created by pulse transmissions from boundary nodes, each boundary node must have the appropriate pulse-connection function. This requirement, however, proves to be extremely problematic and reveals a limitation of the elegant technique of averaging out timing delay when we come to boundaries of the network.

The problem comes because $D_{fix} + D_{j,i}$ already does not have a symmetric distribution if j is a boundary node. Recall that $f_{D_{fix}}(x) = f_{D_j}(-x)$ when j is an interior node and $f_{D_j}(x) = f_{D_l}(x)$ when j and l are both interior nodes. However, $f_{D_j}(x) \neq f_{D_l}(x)$ when j is an interior node and l is a boundary node. As a result, $D_{fix} + D_{j,i}$ is no longer symmetric if j is a boundary node. In fact, it is clear that the distribution of $D_{fix} + D_{j,i}$ is a function of node j's location near the boundary. Because of this additional asymmetry, let us assume for a moment that the sequence of zero-crossings observed by boundary node i occur ϵ_i away from an integer value of t. That is, if every node in the network, including the boundary

nodes, transmitted a sequence of pulses where each pulse was sent according to (34), then boundary node i would observe the sequence of observations

$$\alpha_i(\tau_0 - m + l + \epsilon_i - \bar{\Delta}_i) + \Psi_i, \tag{36}$$

where $l = 0, 1, \ldots, m - 1$ and ϵ_i is known.

This boundary node i could then use the time synchronization estimator given by (32) but where the matrix $\bar{\mathbf{H}}$ is now replaced with $\bar{\mathbf{H}}_i$

$$\bar{\mathbf{H}}_i = \begin{bmatrix} 1 & 1 & 1 & \ldots & 1 \\ \epsilon_i & 1 + \epsilon_i & 2 + \epsilon_i & \ldots & m - 1 + \epsilon_i \end{bmatrix}^T.$$

Thus, for this boundary node i we have

$$V_{n,i}^{c_i}(\mathbf{Y}, \epsilon_i) = \mathbf{C}(\bar{\mathbf{H}}_i^T \bar{\mathbf{H}}_i)^{-1} \bar{\mathbf{H}}_i^T \mathbf{Y}, \tag{37}$$

In this case, however, the variance of the time synchronization estimator depends on ϵ_i

$$\mathrm{Var}_\theta(V_{n,i}^{c_i}(\mathbf{Y}, \epsilon_i)) = \sigma^2 \left(\frac{2(2m+1)}{m(m-1)} + \frac{12\epsilon_i(\epsilon_i - 1 - m)}{(m-1)m(m+1)} \right). \tag{38}$$

The fact that the variance depends on ϵ_i is the root of the problem. The pulse-connection function

$$X_{n,i}^{c_i}(\mathbf{Y}) = V_{n,i}^{c_i}(\mathbf{Y}, \epsilon_i) + \hat{\alpha}_i D_{fix}, \tag{39}$$

is *not* the same as that given by (34).

To correct for this, we can make the strong assumption that each boundary node i knows is own α_i. We address the reasoning behind this assumption in Section V-D. If we use this assumption, then each boundary node i can get an observation sequence of the form (31) simply by adding $\alpha_i(\epsilon - \epsilon_i)$ to each of the m observations of the form given in (36), where we assume that node i knows both ϵ and ϵ_i. With such an observation sequence, boundary node i will have the time synchronization estimator (32) and, more importantly, the pulse-connection function (34). Thus, maintaining time synchronization for the case of propagation delay would be possible.

What we have then is that boundary node synchronization would require only the boundary nodes to know their α_i parameters. With this strong assumption only for the boundary nodes, the network is effectively synchronized. Even though the boundary nodes do not see the same zero-crossing as the interior nodes, they can calculate this time and thus have all the required synchronization information.

D. The Boundary Node Assumption

The assumption that each boundary node i knows α_i is a strong assumption. Even though the fraction of nodes that are boundary nodes is small for multi-hop networks requiring many hops to send information across the network, we believe that the assumption is still very artificial. There are two reasons that we make the assumption for the presentation of results on time synchronization with propagation delay.

First, the assumption allows us to give an elegant presentation of the main concept of this paper which is to use high node density to average out errors in the network. Throughout this work we have used high node density to average out inherent errors present in the nodes. We were able to average out random timing jitter that is present in each node and provide the network with a sequence of zero-crossings that can serve as synchronization events. We then applied this technique to averaging out the errors introduced by time delay. To this end we were partially successful in that the interior nodes can average out these errors assuming the boundary nodes have additional information. But this is of interest since the goal of this paper is to understand the theory of spatial averaging for synchronization and discover its fundamental advantages and limitations.

Second, the problem encountered at the boundaries is one that opens up an entirely new area of study which is the target of our future work. The issue that we encounter is that the waveform seen by some nodes in the network will have a zero-crossing that is shifted from the ideal location. This implies that different nodes will observe different zero-crossings. Furthermore, these zero-crossings will now evolve in time since we do not have the same observations over the entire network. This problem is similar to what we encounter if we consider finite sized networks. For finite N, the zero-crossing location will be random and thus introduce another source of error. As well, different nodes will see different zero-crossing locations. Therefore, we will turn our attention to the case of finite N and develop a different set of tools that will be needed to understand what types of synchronization are achievable under the situation where zero-crossing locations evolve in time. Using this understanding, we hope to return to the issue of propagation delay in asymptotically dense networks and characterize the behavior of the network.

VI. CONCLUSIONS

To conclude, we revisit the scalability issue under the light of work developed in this paper.

A. The Scalability Problem Revisited

In the Introduction (Section I-B.2), we mentioned that most existing proposals for time synchronization suffer from an inherent scalability problem. The problem with those existing proposals lies in the fact that synchronization errors accumulate: if node 2 can synchronize to node 1 with some small error, and node 3 can synchronize to node 2 with the same small error, these errors accumulate, and the synchronization of node 3 to node 1 is worse. Therefore, synchronization error increases with the number of hops in the network, and this problem is especially apparent in the regime of high densities. To make these ideas precise, we first determine the maximum number of hops over which synchronization information must travel and then study how the error in a generic pairwise synchronization mechanism depends on this number of hops.

1) An Estimate of the Maximum Number of Hops: To obtain an estimate for the maximum number of hops ℓ_N in a network in the regime of high densities (fixed area, $N \to \infty$), we approximate the transmission range of a node by the minimum required transmission distance, d_N, to maintain a fully connected network with high probability. From [15], we have that for N nodes uniformly distributed over a $[0,1] \times [0,1]$ square, the graph is connected with probability-1 as $N \to \infty$ if and only if each node's transmission distance d_N is such that

$$\pi d_N^2 = \frac{\log N + \epsilon_N}{N},$$

for some $\epsilon_N \to \infty$. Let us, therefore, approximate d_N as

$$d_N \approx \sqrt{\frac{1}{\pi} \frac{\log N}{N}}.$$

Thus, $\ell_N = 1/d_N = O\left(\sqrt{\frac{N}{\log N}}\right)$, and thus $\ell_N \to \infty$ as $N \to \infty$.

2) Synchronization Error Over Multiple Hops: Now, we assume there are ℓ_N nodes arranged in a linear ordering, numbered 1 to ℓ_N. To synchronize, each node i forms an estimate of its own α_i, based on m pulses transmitted from node $i - 1$. As before, node 1 will have the reference clock $c_1(t) = t$.

Node 1 starts by sending m pulses at times $\tau_1 + l$ for $l = 0, 1, \ldots, m - 1$. As a result, node 2 will get a vector of observations $\mathbf{Y}_2$, where $\mathbf{Y}_2[1] = \alpha_2(\tau_1 - \bar{\Delta}_2) + \Psi_2$ and the $(l+1)$th element of $\mathbf{Y}_2$ is $\mathbf{Y}_2[l+1] = \alpha_2(\tau_1 - \bar{\Delta}_2) + l\alpha_2 + \Psi_2$. This is similar to the situation we had in (19) and we can therefore estimate α_2 using

$$\hat{\alpha}_2 = \bar{\mathbf{C}}(\mathbf{H}^T\mathbf{H})^{-1}\mathbf{H}^T\mathbf{Y}_2,$$

where $\bar{\mathbf{C}} = \begin{bmatrix} 0 & 1 \end{bmatrix}$. We find that $\hat{\alpha}_2 \sim \mathcal{N}(\alpha_2, 12\sigma^2/((m-1)m(m+1)))$.

Node 2 will now transmit m pulses at times, in terms of c_2, $\bar{\tau}_2 + l\hat{\alpha}_2$, for $l = 0, 1, \ldots, m - 1$. Note that $\hat{\alpha}_2$ is now a fixed value since node 2 has estimated α_2. In terms of c_1, these pulses occur at

$$(\bar{\tau}_2 + l\hat{\alpha}_2)^{c_1} = \frac{\bar{\tau}_2 + l\hat{\alpha}_2 - \Psi_2}{\alpha_2} + \bar{\Delta}_2 = \tau_2 + l\frac{\hat{\alpha}_2}{\alpha_2} - \frac{\Psi_2}{\alpha_2},$$

for $l = 0, 1, \ldots, m - 1$, where $\tau_2 = (\bar{\tau}_2/\alpha_2) + \bar{\Delta}_2$. Thus, if we translate these times into the time scale of c_3, we will have the vector of observations, $\mathbf{Y}_3$, made by node 3. We find that the $(l + 1)$th element of $\mathbf{Y}_3$ is

$$\mathbf{Y}_3[l + 1] = \alpha_3((\tau_2 + l\frac{\hat{\alpha}_2}{\alpha_2} - \frac{\Psi_2}{\alpha_2}) - \bar{\Delta}_3) + \Psi_3 \sim \mathcal{N}\left(\alpha_3(\tau_2 - \bar{\Delta}_3) + l\alpha_3\frac{\hat{\alpha}_2}{\alpha_2}, \sigma^2\left(\frac{\alpha_3^2}{\alpha_2^2} + 1\right)\right).$$

This vector of observations is of the form

$$\mathbf{Y}_3 = \mathbf{H}\bar{\theta} + \bar{\mathbf{W}}, \tag{40}$$

where

$$\bar{\theta} = \begin{bmatrix} \bar{\theta}_1 \\ \bar{\theta}_2 \end{bmatrix} = \begin{bmatrix} \alpha_3(\tau_2 - \bar{\Delta}_3) \\ \alpha_3\frac{\hat{\alpha}_2}{\alpha_2} \end{bmatrix}$$

with

$$\mathbf{H} = \begin{bmatrix} 1 & 1 & 1 & \ldots & 1 \\ 0 & 1 & 2 & \ldots & m - 1 \end{bmatrix}^T$$

and $\mathbf{W} = [W_1 \ldots W_m]^T$. $\mathbf{W} \sim \mathcal{N}(0, \Sigma)$ with $\Sigma = \sigma^2\left(\frac{\alpha_3^2}{\alpha_2^2} + 1\right)\mathbf{I}$.

With this vector of observations, we can use the estimator

$$\hat{\alpha}_3 = \bar{\mathbf{C}}(\mathbf{H}^T\mathbf{H})^{-1}\mathbf{H}^T\mathbf{Y}_3,$$

where $\bar{\mathbf{C}} = [0 \quad 1]$. We find that

$$\hat{\alpha}_3 \sim \mathcal{N}\left(\alpha_3\frac{\hat{\alpha}_2}{\alpha_2}, \frac{12\sigma^2}{((m - 1)m(m + 1))}\left(\frac{\alpha_3^2}{\alpha_2^2} + 1\right)\right).$$

If we continue this reasoning, we find that

$$\hat{\alpha}_{\ell_N} \sim \mathcal{N}\left(\alpha_{\ell_N}\frac{\hat{\alpha}_{\ell_N-1}}{\alpha_{\ell_N-1}}, \frac{12\sigma^2}{((m - 1)m(m + 1))}\left(\frac{\alpha_{\ell_N}^2}{\alpha_{\ell_N-1}^2} + 1\right)\right)$$

will be the estimate of node ℓ_N.

From the above analysis, we see that each node i's estimate suffers from jitter variance of the same form. However, there is an accumulation of error because node i's estimate has a mean that is dependent on node $i-1$'s estimate. As a result, if node $i-1$ has some small error, then that error will propagate to the estimate of node i. A good way to see this is if we consider the special case where $\alpha_2 = \alpha_3 = \ldots \alpha_{\ell_N} = 1$.

This is the case where the clock frequencies are the same, but nodes do not know this. In this case, we find that node ℓ_N's estimate can be written as

$$\hat{\alpha}_{\ell_N} = \hat{\alpha}_2 + \sum_{i=3}^{\ell_N} W_i, \qquad \ell_N \geq 2$$

where $W_i \sim \mathcal{N}(0, 24\sigma^2/((m-1)m(m+1)))$. This is intuitively obvious because node i's estimate $\hat{\alpha}_i$ will be the mean of the Gaussian random variable $\hat{\alpha}_{i+1}$. Therefore, it is obvious that the error variance grows linearly with the number of hops. In fact, this behavior is observed in experimental work. With Reference Broadcast Synchronization (RBS), from [8] the authors find that the synchronization error variance of an ℓ_N hop path is approximately $\sigma^2 \ell_N$, where σ^2 is the one hop error variance. Therefore, we have that the synchronization error between our two nodes will grow linearly as $\ell_N = 1/d_N$, which is strictly monotonically increasing. As a result, as $N \to \infty$, we have that synchronization error will grow unbounded.

This scalability problem, however, can potentially be avoided using cooperative time synchronization as $N \to \infty$. This is because in the limit of infinite density, the cooperative time synchronization technique allows every node in the network to see a set of identical equispaced zero-crossings. As a result, in steady-state the synchronization error does not grow across the network. This comes about by using the high node density to average out random timing errors. Thus, we find that cooperative time synchronization has very favorable scalability properties in the limit as $N \to \infty$.

B. Network Density and Synchronization Performance Trade-Off

The cooperative synchronization technique described in this paper provides us deterministic parameters that we can use for time synchronization in the limit as node density grows unbounded. In fact, as the node density grows, the observations that can be used for synchronization improve. This means that our cooperative synchronization technique provides an effective trade-off between network density and synchronization performance. Such a trade-off has not existed before and will provide network designers an additional dimension over which to improve network synchronization performance.

The fundamental idea behind cooperative time synchronization is that by using spatial averaging, the errors inherent in each node can be averaged out. By using observations that are an "average" of the information from a large number of surrounding nodes, synchronization performance can be improved due to the higher quality observations.

From this point of view, it is clear that the particular technique described in this paper is but one example of using spatial averaging to improve synchronization. Other techniques can also be developed

using spatial averaging. For example, nodes may not necessarily have to send odd-shaped pulses and use zero-crossing observations. Even though this setup takes advantage of the superposition of pulses, it has its drawbacks. To keep the signals in phase, the jitter variance will limit the maximum frequency at which signals can be sent. Instead, nodes may transmit ultra wideband pulses. If the nodes surrounding a particular node j each transmit an impulse at their estimate of an integer value of t, then due to timing errors in the surrounding nodes, node j will see a cluster of pulse arrivals around this integer value of t. Node j can then take the sample mean of this cluster of pulses and use that as an observation, just like we used the zero-crossing as an observation in this paper. This idea is illustrated in Fig. 8. Such a technique based on ultra wideband pulses will also provide similar scalability properties. As a result, cooperative time synchronization really describes a class of techniques that can take advantage of spatial averaging to improve synchronization performance.
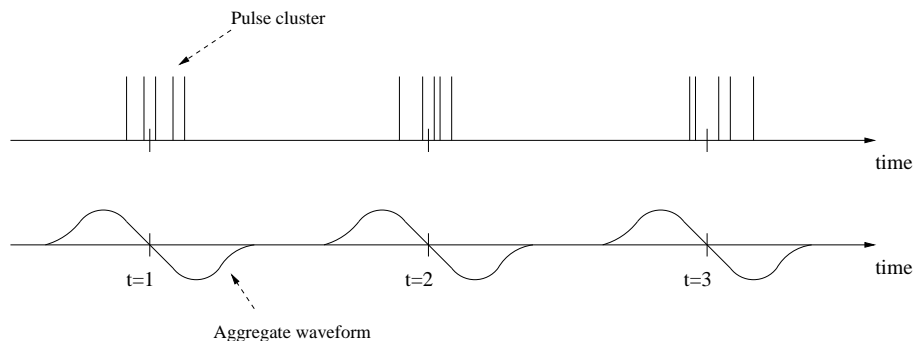

Fig. 8. Clusters of ultra wideband pulses can be used for cooperative time synchronization. In the the top figure, we illustrate the clusters of pulses around integer values of t. As the number of nodes increase, the sample mean will converge to the integer value of the reference time. This idea is parallel to the use of zero-crossings shown in the bottom figure.

C. Future Work

With the goal of developing practical cooperative synchronization mechanisms, two keys areas of interest are cooperative synchronization in finite-sized networks and algorithm development. First, the analysis of performance for finite-sized networks is very important. Determining when the asymptotic properties presented in this work are good predictors of performance in networks that may be large but still finite in size is important in terms of bridging the gap between our proposed ideas and practical systems. Preliminary, simulation-based work along these lines can be found in [19]. Second, developing practical techniques for cooperative time synchronization is essential for implementing spatial averaging

in real networks. Along these lines, one area of interest is determining what types of pulses should be used, i.e. odd-shaped pulses or ultra wideband pulses.

Furthermore, the ideas in this paper suggest a few other areas of interest for future work. One is the issue of distributed modulation methods. If we have the ability to generate an aggregate waveform with equispaced zero-crossings, by controlling the location of these crossings we can modulate information onto this waveform and use it to communicate with a far receiver. Preliminary work along these lines can be found in [20]. Another issue is to study how the idea of spatial averaging that is so prevalent in this work contributes to synchronization that is observed in nature.

APPENDIX

Proof of Lemma 1.   To show (12), we consider

$$
\begin{aligned}
E(A_{max}K_i p(\tau_1 - \tau_0 - T_i)) &= A_{max} E(K_i) E(p(\tau_1 - \tau_0 - T_i)) \\
&= A_{max} E(K_i) \int p(\tau_1 - \tau_0 - \psi) f_{T_i}(\psi) d\psi \\
&= -A_{max} E(K_i) \int p(\psi - (\tau_1 - \tau_0)) f_{T_i}(\psi) d\psi
\end{aligned}
$$

Since $\tau_1 < \tau_0$, we have that $\tau_1 - \tau_0 < 0$ implying that $p(\psi)$ is shifted to the left and the zero-crossing of $p(\psi)$ occurs at a negative value. $p(\psi)$ is odd about its zero-crossing and $f_{T_i}(\psi)$ is symmetric about zero and strictly monotonically increasing on $(-\infty, 0]$ for all positive finite variance values. Thus, it is clear that $\int p(\psi - (\tau_1 - \tau_0)) f_{T_i}(\psi) d\psi < 0$ which makes $E(A_{max}K_i p(\tau_1 - \tau_0 - T_i)) > 0$.

Now, the expectation will vary with the variance of T_i and the variance will range from a positive upper bound of $\bar{\sigma}^2 / \alpha_{low}^2 < B$ to a positive lower bound of $\bar{\sigma}^2 / \alpha_{up}^2$, where recall that $\bar{\sigma}^2$ is a value determined by our choice of the pulse connection function. If we consider $\int p(\psi - (\tau_1 - \tau_0)) f_{T_i}(\psi) d\psi$ to be a function of the variance of T_i, then we see that it is bounded and continuous on the compact domain $[\bar{\sigma}^2 / \alpha_{up}^2, \bar{\sigma}^2 / \alpha_{low}^2]$. Since we showed in the previous paragraph that $E(A_{max}K_i p(\tau_1 - \tau_0 - T_i)) > 0$ whenever T_i has a nonzero finite variance, clearly $E(A_{max}K_i p(\tau_1 - \tau_0 - T_i)) > 0$ when $\mathrm{Var}(T_i) \in [\bar{\sigma}^2 / \alpha_{up}^2, \bar{\sigma}^2 / \alpha_{low}^2]$. Thus, it is clear that γ_1 and γ_2 exist and (12) is shown.

To show (13), we consider

$$
\begin{aligned}
\mathrm{Var}(A_{max}K_i p(\tau_1 - \tau_0 - T_i)) &= E(A_{max}^2 K_i^2 p^2(\tau_1 - \tau_0 - T_i)) - E^2(A_{max}K_i p(\tau_1 - \tau_0 - T_i)) \\
&\leq A_{max}^2 E(K_i^2) E(p^2(\tau_1 - \tau_0 - T_i)) \\
&\leq A_{max}^2 E(K_i^2) \\
&\leq A_{max}^2
\end{aligned}
$$

where the second to last inequality follows from the fact that $E(p^2(\tau_1 - \tau_0 - T_i))$ is upper bounded by 1. The last inequality follows since $E(K_i^2) \leq 1$ by the fact that $0 \leq K_i \leq 1$. Thus, we have shown (13).

Next we define $S_n = \bar{M}_1(\tau_1) + \cdots + \bar{M}_n(\tau_1)$ and $m_n = E(S_n) = \mu_1 + \ldots + \mu_n$. From [10] we have the following theorem

Theorem 3: The convergence of the series

$$
\sum \frac{\sigma_i^2}{i^2}
$$

implies that the strong law of large numbers will apply to the sequence of independent random variables $\bar{M}_i(\tau_1)$. That is, again from [10], for every pair $\epsilon > 0$, $\delta > 0$, there corresponds an N such that

$$\Pr\left\{\frac{|S_n - m_n|}{n} < \epsilon; \quad n = N, N+1, \ldots, N+r\right\} > 1 - \delta$$

for all $r > 0$. $\triangle$

We have shown (13) so we have $\sigma_i^2 < \gamma_3 < \infty$. Thus

$$\lim_{N \to \infty} \sum_{i=1}^{N} \frac{\sigma_i^2}{i^2} \leq \lim_{N \to \infty} \sum_{i=1}^{N} \frac{\gamma_3}{i^2} = \gamma_3 \frac{\pi^2}{6}.$$

and we have convergence by the direct comparison test. Therefore, we can apply Theorem 3 and get that for any pair $\epsilon > 0$, $\delta > 0$, we can find an N such that

$$\Pr\left\{\left|\frac{S_n}{n} - \frac{m_n}{n}\right| < \epsilon; \quad n = N, N+1, \ldots, N+r\right\} > 1 - \delta \tag{41}$$

for all $r > 0$.

By (12) we have that $\gamma_2 > \mu_i > \gamma_1 > 0$. Thus, we can clearly see that

$$\frac{m_n}{n} > \gamma_1.$$

Furthermore, since we keep the function $f_\alpha(s)$ constant as we increase the number of nodes in the network we get that m_n/n converges to a constant $\eta(\tau_1)$ given by

$$\begin{aligned}
\eta(\tau_1) &= A_{max} E(K_i) \int_{\alpha_{low}}^{\alpha_{up}} \int_{-\infty}^{\infty} p(\tau_1 - \tau_0 - \psi) f_T(\psi, s) d\psi f_\alpha(s) ds \\
&= \int_{\alpha_{low}}^{\alpha_{up}} E(\bar{M}_i(\tau_1, s)) f_\alpha(s) ds.
\end{aligned}$$

The above expression comes from the fact that since each $\mu_i = E(\bar{M}_i(\tau_1))$ is a function of α_i, m_n/n will converge to the average of the μ_i over $f_\alpha(s)$, the function that characterizes the set of α_i's. Therefore, given any ϵ, we can find an N' such that

$$\left|\frac{m_n}{n} - \eta(\tau_1)\right| < \epsilon \tag{42}$$

for all $n > N'$. Note that since $(m_n/n) > \gamma_1$, we have that $\eta(\tau_1) \geq \gamma_1$. Since

$$\left|\frac{S_n}{n} - \eta(\tau_1)\right| < \left|\frac{S_n}{n} - \frac{m_n}{n}\right| + \left|\frac{m_n}{n} - \eta(\tau_1)\right|,$$

using (41) and (42) we have

$$\Pr\left\{\left|\frac{S_n}{n} - \eta(\tau_1)\right| < 2\epsilon; \quad n = N'', N''+1, \ldots, N''+r\right\} > 1 - \delta.$$

for all $r > 0$, where $N'' = \max\{N, N'\}$. Thus, we have

$$\lim_{N \to \infty} \frac{1}{N} \sum_{i=1}^{N} \bar{M}_i(\tau_1) = \eta(\tau_1) > 0$$

almost surely. This completes the proof of Lemma 1. $\quad\triangle$

Proof of Lemma 3. First, we start by finding an analytical expression for $|A_\infty(t) - A_\infty(t_o)|$. From the proof of Lemma 1 we have that

$$A_\infty(t) = A_{max}E(K_i) \int_{\alpha_{low}}^{\alpha_{up}} \int_{-\infty}^{\infty} p(t - \tau_0 - \psi)f_T(\psi, s)d\psi f_\alpha(s)ds.$$

Therefore, $|A_\infty(t) - A_\infty(t_o)|$ can be written as

$$
\begin{aligned}
&|A_\infty(t) - A_\infty(t_o)| \\
&= \left| A_{max}E(K_i) \int_{\alpha_{low}}^{\alpha_{up}} \int_{-\infty}^{\infty} [p(t - \tau_o - \psi) - p(t_o - \tau_o - \psi)]f_T(\psi, s)f_\alpha(s)d\psi ds \right| \\
&\leq A_{max} \int_{\alpha_{low}}^{\alpha_{up}} \int_{-\infty}^{\infty} |p(t - \tau_o - \psi) - p(t_o - \tau_o - \psi)|f_T(\psi, s)f_\alpha(s)d\psi ds \\
&= A_{max} \int_{\alpha_{low}}^{\alpha_{up}} \int_{-\tau_{nz}+t_o-\tau_0-|t-t_o|}^{\tau_{nz}+t_o-\tau_0+|t-t_o|} |p(t - \tau_o - \psi) - p(t_o - \tau_o - \psi)|f_T(\psi, s)f_\alpha(s)d\psi ds,
\end{aligned}
$$

where $E(K_i) \leq 1$. The change in the limits of integration in the last equality comes from the fact that $p(t - \tau_o - \psi) - p(t_o - \tau_o - \psi) = 0$ outside of $\psi \in [-\tau_{nz} + t_o - \tau_0 - |t - t_o|, \tau_{nz} + t_o - \tau_0 + |t - t_o|]$. This is the maximum interval over which $p(t - \tau_o - \psi) - p(t_o - \tau_o - \psi)$ can be non-zero. There is no need to take the absolute value of $f_T(\psi, s)$ and $f_\alpha(s)$ since they are always non-negative.

Our second step is to bound the inner integral. Before doing so, we first show that the inside integral is in fact Riemann integrable. For any given t and t_o, the inside integral is taken over a closed interval. Over a closed interval, we know from Strichartz [39] that any bounded function that is continuous except at a finite number of points is Riemann integrable. Furthermore, also from [39] we know that the sums and products of continuous functions are continuous. As well, if a function is continuous then the absolute value of that function is also continuous. $p(t)$ has at most $D = 3$ locations at which it is discontinuous and over any open interval not containing a discontinuity, $p(t)$ is uniformly continuous since $q(t)$ is uniformly continuous. $f_T(\psi, s)$ has $D' = 0$ discontinuities in ψ for an given s since it is Gaussian for any s. And since $s \in [\alpha_{low}, \alpha_{up}]$, $|f_T(\psi, s)| \leq G_T$ for all ψ and s (G_T occurring when $\psi = 0$ and $s = \alpha_{up}$). Thus, since $p(t)$ and $f_T(\psi, s)$ are continuous except at a finite number of points, we see that for given s, t, and t_0

$$|p(t - \tau_o - \psi) - p(t_o - \tau_o - \psi)|f_T(\psi, s)$$

is also continuous in ψ except at a finite number of points (at most $D' + 2D$ points). This function is also bounded since the product of two bounded functions is bounded. As a result, we see that the integral is Riemann integrable over any closed interval.

We now proceed to bound from above the value of this integral by first bounding the maximum value of the integral assuming no discontinuities and then introducing another term that bounds the maximum area contributed by the discontinuities. If we ignore the discontinuities and assume $p(t)$ is uniformly continuous, for any $m_1 > 0$ there exists a $n > 0$ such that

$$|t - t_o| < \frac{1}{n} \Rightarrow |p(t) - p(t_o)| < \frac{1}{m_1},$$

for all t and t_o. As a result, $p(t - \tau_o - \psi) - p(t_o - \tau_o - \psi)$ can be made as small as desired by choosing the proper n thus giving us $p(t - \tau_o - \psi) - p(t_o - \tau_o - \psi) < 1/m_1$ for all ψ for an appropriate choice of n.

Furthermore, we note that $|p(t - \tau_o - \psi)| f_T(\psi, s) \leq G_T$ because $|p(t)| \leq 1$ and $|f_T(\psi, s)| \leq G_T$. The maximum possible jump at a discontinuity in the function $|p(t - \tau_o - \psi) - p(t_o - \tau_o - \psi)| f_T(\psi, s)$ is thus $2G_T$ and for any $|t - t_o|$, the maximum area contributed by each discontinuity is $2G_T |t - t_o|$. As a result, for all $D' + 2D$ discontinuities, the maximum area contribution will be no more than $2G_T |t - t_o|(D' + 2D)$.

We can, therefore, bound the inner integral as

$$\int_{-\tau_{nz}+t_o-\tau_0-|t-t_o|}^{\tau_{nz}+t_o-\tau_0+|t-t_o|} |p(t - \tau_o - \psi) - p(t_o - \tau_o - \psi)| f_T(\psi, s) d\psi$$

$$\leq \int_{-\tau_{nz}+t_o-\tau_0-|t-t_o|}^{\tau_{nz}+t_o-\tau_0+|t-t_o|} \frac{G_T}{m_1} d\psi + 2G_T |t - t_o|(D' + 2D)$$

$$= \frac{G_T}{m_1}(2\tau_{nz} + 2|t - t_o|) + 2G_T |t - t_o|(D' + 2D)$$

$$= 2\frac{G_T}{m_1}\tau_{nz} + 2\frac{G_T}{m_1}|t - t_o| + 2G_T |t - t_o|(D' + 2D),$$

where $|t - t_o| < 1/n$.

What we have is that if $|t - t_0| < 1/n$ then

$$|A_\infty(t) - A_\infty(t_o)|$$

$$\leq A_{max} \int_{\alpha_{low}}^{\alpha_{up}} \left(2\frac{G_T}{m_1}\tau_{nz} + 2\frac{G_T}{m_1}|t - t_o| + 2G_T |t - t_o|(D' + 2D)\right) f_\alpha(s) ds$$

$$\leq A_{max} G_\alpha(\alpha_{up} - \alpha_{low}) \left(2\frac{G_T}{m_1}\tau_{nz} + 2\frac{G_T}{m_1}|t - t_o| + 2G_T |t - t_o|(D' + 2D)\right)$$

since $|f_\alpha(s)| < G_\alpha$ (defined in Section III-A). We define $\bar{A}$ as

$$\bar{A} = A_{max} G_\alpha(\alpha_{up} - \alpha_{low}).$$

Now, for the third step of our proof we make

$$|A_\infty(t) - A_\infty(t_o)|$$
$$\leq \quad \bar{A}\left(2\frac{G_T}{m_1}\tau_{nz} + 2\frac{G_T}{m_1}|t - t_o| + 2G_T|t - t_o|(D' + 2D)\right)$$
$$< \quad \frac{1}{m},$$

for any choice of $m > 0$. We do this by making each of the three terms less than $1/(3m)$.

For the first term we want

$$\frac{2\bar{A}G_T\tau_{nz}}{m_1} < \frac{1}{3m}.$$

We solve and get

$$m_1 > 6m\bar{A}G_T\tau_{nz}.$$

Since for any value of $m_1 > 0$ we can find an $n > 0$, this condition can be satisfied.

For the third term we want

$$2\bar{A}G_T(D' + 2D)|t - t_o| < \frac{1}{3m}.$$

This gives us

$$|t - t_o| < \frac{1}{6\bar{A}G_T(D' + 2D)m}.$$

Since the only requirement is $|t - t_o| < 1/n$ for n chosen by any given $m_1 > 0$, we can always choose $|t - t_o|$ as small as desired. Thus, this condition can be satisfied.

With the second term we want the condition

$$\frac{2\bar{A}G_T}{m_1}|t - t_o| < \frac{1}{3m}$$

which means that

$$\frac{|t - t_o|}{m_1} < \frac{1}{6m\bar{A}G_T}.$$

Again, this condition can be satisfied since we can choose m_1 as large as we want and $|t - t_o|$ as small as we want as long as $|t - t_o| < 1/n$ for a given m_1.

Thus, for any $m > 0$, we first choose $m_1 > 6m\bar{A}G_T\tau_{nz}$. Then, we find an $n' > 0$ such that $|t - t_o| < 1/n'$ implies that $|p(t) - p(t_o)| < 1/m_1$ for all t and t_o if we remove the discontinuities in $p(t)$. Then, if necessary, n' is increased to n so that $|t - t_o| < 1/n$ implies that $|t - t_o| < 1/(6\bar{A}G_T(D' + 2D)m)$ and $|t - t_o|/m_1 < 1/(6m\bar{A}G_T)$. If no increase is necessary, then $n = n'$. With this choice of $n > 0$, $|A_\infty(t) - A_\infty(t_o)| < 1/m$. As a result, for any m, we can find an n such that $|t - t_o| < 1/n$ implies that $|A_\infty(t) - A_\infty(t_o)| < 1/m$. Thus, $A_\infty(t)$ is continuous.

This completes the proof for Lemma 3. $\triangle$

Proof of Theorem 2. Let us start by writing (30) as

$$A_{j,N}^{c_1}(t) = \sum_{i=1}^{N} \frac{A_{max}K_{fix}K_{j,i}}{N}p(t - \tau_o - T_i - D_{fix} - D_{j,i}) = \sum_{i=1}^{N} \frac{1}{N}\tilde{M}_i(t,s),$$

where $\tilde{M}_i(t,s) \triangleq A_{max}K_{fix}K_{j,i}p(t - \tau_o - T_i - D_{fix} - D_{j,i})$. Recall that the dependence on s comes from the fact that the density of T_i is a function of α_i which is characterized by $f_\alpha(s)$. This notation is analogous to the notation used in Section III-C. Following the steps in the proof of Lemma 1, we can quickly show that the limiting aggregate waveform at node j will take on the form

$$\eta(t) = \int_{\alpha_{low}}^{\alpha_{up}} E(\tilde{M}_i(t,s))f_\alpha(s)ds, \tag{43}$$

where

$$E(\tilde{M}_i(t,s))$$
$$= A_{max}\int_{-\infty}^{\infty}\int_{-\infty}^{0}\int_{0}^{\infty} g(-y)g(x)p(t - \tau_0 - \psi - y - x)f_{D_j}(x)f_{D_{fix}}(y)f_T(\psi,s)dxdyd\psi,$$

with $g(\cdot) = K(\delta^{-1}(\cdot))$. Therefore, we can prove Theorem 2 in two steps:

- To show that $\eta(t)$ is odd about τ_0, we need to show that $E(\tilde{M}_i(t,s))$ is odd in t about τ_0, i.e. $E(\tilde{M}_i(\tau_0 + \xi, s)) = -E(\tilde{M}_i(\tau_0 - \xi, s))$ for $\xi \geq 0$.

- To show a zero-crossing at τ_0, show that $E(\tilde{M}_i(\tau_0, s)) = 0$.

These two steps come directly from the form of $\eta(t)$ in (43).

We first show that $E(\tilde{M}_i(\tau_0 + \xi, s)) = -E(\tilde{M}_i(\tau_0 - \xi, s))$ for $\xi \geq 0$. Using the fact that $K_{fix} = K(\delta^{-1}(-D_{fix})) = g(-D_{fix})$ and $K_{j,i} = g(D_{j,i})$, we have the following:

$$E(\tilde{M}_i(\tau_0 + \xi, s))$$
$$= E\big(A_{max}g(-D_{fix})g(D_{j,i})p(\xi - [T_i + D_{fix} + D_{j,i}])\big)$$
$$\overset{(a)}{=} -E\big(A_{max}g(-D_{fix})g(D_{j,i})p(-\xi + [T_i + D_{fix} + D_{j,i}])\big)$$
$$= -A_{max}\int_{-\infty}^{\infty}\int_{-\infty}^{0}\int_{0}^{\infty} g(-y)g(x)p(-\xi + [\psi + y + x])f_{D_j}(x)f_{D_{fix}}(y)f_T(\psi,s)dxdyd\psi$$
$$\overset{(b)}{=} A_{max}\int_{\infty}^{-\infty}\int_{\infty}^{0}\int_{0}^{-\infty} g(z)g(-u)p(-\xi - [w + z + u])f_{D_j}(-u)f_{D_{fix}}(-z)f_T(-w,s)dudzdw$$
$$\overset{(c)}{=} -A_{max}\int_{-\infty}^{\infty}\int_{-\infty}^{0}\int_{0}^{\infty} g(-u)g(z)p(-\xi - [w + u + z])f_{D_j}(z)f_{D_{fix}}(u)f_T(w,s)dzdudw$$
$$= -E\big(A_{max}g(-D_{fix})g(D_{j,i})p(-\xi - [T_i + D_{fix} + D_{j,i}])\big)$$
$$= -E(\tilde{M}_i(\tau_0 - \xi, s)),$$

where (a) follows because $p(t) = -p(-t)$ and at (b) we did a change of variables with $u = -x$, $w = -\psi$, and $z = -y$. (c) follows from $f_T(x, s) = f_T(-x, s)$ and $f_{D_j}(x) = f_{D_{fix}}(-x)$. We thus have $E(\tilde{M}_i(\tau_0 + \xi, s)) = -E(\tilde{M}_i(\tau_0 - \xi, s))$ for $\xi \geq 0$.

$E(\tilde{M}_i(\tau_0, s)) = 0$ can now be shown as follows. Using the just proven fact that $E(\tilde{M}_i(\tau_0 + \xi, s)) = -E(\tilde{M}_i(\tau_0 - \xi, s))$ for $\xi \geq 0$, setting $\xi = 0$ gives us $E(\tilde{M}_i(\tau_0, s)) = -E(\tilde{M}_i(\tau_0, s))$. This implies that $E(\tilde{M}_i(\tau_0, s)) = 0$.

This completes the proof for Theorem 2. $\triangle$

REFERENCES

[1] A. Ledeczi, P. Volgyesi, M. Maroti, G. Simon, G. Balogh, A. Nadas, B. Kusy, S. Dora and G. Pap. Multiple Simultaneous Acoustic Source Localization in Urban Terrain. In *Proc. Information Processing in Sensor Networks (IPSN'05)*, Los Angeles, CA, 2005.

[2] J. Buck and E. Buck. Synchronous Fireflies. *Scientific American*, 234:74-85, 1976.

[3] C. Chen. Threshold Effects on Synchronization of Pulse-Coupled Oscillators. *Physical Review E*, 49(4):2668-2672, 1994.

[4] A. Corral, C. J. Pérez, A. Díaz-Guilera and A. Arenas. Self-Organized Criticality and Synchronization in a Lattice Model of Integrate-and-Fire Oscillators. *Physical Review Letters*, 74(1):118-121, 1995.

[5] A. Díaz-Guilera, C. J. Pérez and A. Arenas. Mechanism of Synchronization and Pattern Formation in a Lattice of Pulse-Coupled Oscillators. *Physical Review E*, 57(4):3820-3828, 1998.

[6] B. Barriac, R. Mudumbai and U. Madhow. Distributed Beamforming for Information Transfer in Sensor Networks. In *Proc. International Symposium on Information Processing in Sensor Networks (IPSN)*, Berkeley, CA, 2004.

[7] H. Ochiai, P.Mitran, H. V. Poor and V. Tarokh. Collaborative Beamforming for Distributed Wireless Ad Hoc Sensor Networks. *IEEE Transactions on Signal Processing*, 53(11):4110-4124, 2005.

[8] J. Elson, L. Girod, and D. Estrin. Fine-Grained Network Time Syncrhonization using Reference Broadcasts. In *Proc. 5th Symp. Op. Syst. Design Implementation (OSDI)*, Boston, MA, 2002.

[9] U. Ernst, K. Pawelzik and T. Geisel. Delay-Induced Multistable Synchronization of Biological Oscillators. *Physical Review E*, 57(2):2150-2162, 1998.

[10] W. Feller. *An Introduction to Probability Theory and its Applications*. John Wiley & Sons, Inc., 1968.

[11] S. Ganeriwal, R. Kumar and M. B. Srivastava. Timing-Sync Protocol for Sensor Networks. In *Proc. First ACM Conference on Embedded Networked Sensor Systems (SenSys)*, Los Angeles, CA, November 2003.

[12] W. Gerstner. Rapid Phase Locking in Systems of Pulse-Coupled Oscillators with Delays. *Physical Review Letters*, 76(10):1755-1758, 1996.

[13] J. van Greunen and J. Rabaey. Lightweight Time Synchronization for Sensor Networks. In *Proc. 2nd ACM International Workshop on Wireless Sensor Networks and Applications (WSNA 2003)*, San Diego, CA, September 2003.

[14] X. Guardiola, A. Díaz-Guilera, M. Llas and C. J. Pérez. Synchronization, Diversity, and Topology of Networks of Integrate and Fire Oscillators. *Physical Review E*, 62(4):5565-5570, 2000.

[15] P. Gupta and P. R. Kumar. Critical Power for Asymptotic Connectivity in Wireless Networks. In W. M. McEneany, G. Yin, and Q. Zhang, editors, *Stochastic Analysis, Control, Optimization and Applications: A Volume in Honor of W. H. Fleming*. Birkhauser, 1998.

[16] A. Herz and J. J. Hopfield. Earthquake Cycles and Neural Reverberations: Collective Oscillations in Systems with Pulse-Coupled Threshold Elements. *Physical Review Letters*, 75(6):1222-1225, 1995.

[17] Y. Hong and A. Scaglione. A Scalable Synchronization Protocol for Large Scale Sensor Networks and its Applications. *IEEE Journal on Selected Areas in Communications (JSAC)*, 23(5):1085-1099, May 2005.

[18] G. Werner-Allen, G. Tewari, A. Patel, M. Welsh, and R. Nagpal. Firefly-Inspired Sensor Network Synchronicity with Realistic Radio Effects. In *Proc. SenSys'05*, San Diego, CA, November 2005.

[19] A. Hu and S. D. Servetto. Algorithmic Aspects of the Time Synchronization Problem in Large-Scale Sensor Networks. ACM/Kluwer Mobile Networks and Applications. Special Issue on Wireless Sensor Networks. 10:491-503, 2005.

[20] A. Hu and S. D. Servetto. dFSK: *Distributed* Frequency Shift Keying Modulation in Dense Sensor Networks. In *Proc. IEEE Int. Conf. Commun. (ICC)*, Paris, France, 2004.

[21] E. M. Izhikevich. Weakly Pulse-Coupled Oscillators, FM Interations, Synchronization, and Oscillatory Associative Memory. *IEEE Trans. Neural Networks*, 10(3):508-526, 1999.

[22] J. Jalife. Mutual Entrainment and Electrical Coupling as Mechanisms for Synchronous Firing of Rabbit Sinoatrial Pacemaker Cells. *J. Physiol.*, 356:221-243, 1984.

[23] S. M. Kay. *Fundamentals of Statistical Signal Processing: Estimation Theory*. PTR Prentice Hall, Inc., 1993.

[24] C. Kelly IV, V. Ekanayake, and R. Manohar. SNAP: A Sensor Network Asynchronous Processor. In *Proc. 9th Int. Symp. Async. Circ. Syst.*, Vancouver, BC, 2003.

[25] Y. Kuramoto. Collective Synchronization of Pulse-Coupled Oscillators and Excitable Units. *Physica D*, 50:15-30, 1991.

[26] L. Lamport. Time, Clocks, and the Ordering of Events in a Distributed System. *Comm. ACM*, 21(4):558–565, 1978.

[27] H. Li, A. Lal, J. Blanchard, and D. Henderson. Self-Reciprocating Radioisotope-Powered Cantilever. *J. Applied Phys.*, 92(2):1122–1127, 2002.

[28] D. Lucarelli and I. Wang. Decentralized Synchroniztion Protocols with Nearest Neighbor Communication. In *Proc. SenSys'04*, Baltimore, Maryland, 2004.

[29] M. Maroti, B. Kusy, G. Simon and A. Ledeczi. The Flooding Time Synchronization Protocol. In *Proc. 2nd International Conference on Embedded Neteworked Sensor Systems*, Baltimore, MD, November 2004.

[30] R. Mathar and J. Mattfeldt. Pulse-Coupled Decentral Synchronization. *SIAM Journal on Applied Mathematics*, 56(4):1094-1106, 1996.

[31] M. K. McClintock Menstrual Synchrony and Suppression. *Nature*, 229:244-245, 1971.

[32] R. E. Mirollo and S. H. Strogatz. Synchronization of Pulse-Coupled Biological Oscillators. *SIAM J. Appl. Math.*, 50(6):1645–1662, 1990.

[33] H. V. Poor. *An Introduction to Signal Detection and Estimation*. Springer-Verlag, 1994.

[34] N. Roberts. Phase Noise and Jitter: A Primer for Digital Designers. `http://www.eedesign.com/showArticle.jhtml?articleID=16501598`, 2003.

[35] A. Sherman, J. Rinzel and J. Keizer. Emergence of Organized Bursting in Clusters of Pancreatic Beta-Cells by Channel Sharing. *Biophys. J.*, 54:411-425, 1988.

[36] M. L. Sichitiu and C. Veerarittiphan. Simple, Accurate Time Synchronization for Wireless Sensor Networks. In *Proc. IEEE Wireless Communication and Networking Conference (WCNC 2003)*, New Orleans, LA, March 2003.

[37] L. S. Smith, D. E. Cairns and A. Nschwitz. Synchronization of Integrate-and-Fire Neurons with Delayed Inhibitory Lateral Connections. In *Proc. International Conference on Artificial Neural Networks (ICANN)*, 1994.

[38] H. Stark and J. Woods. *Probability, Random Processes, and Estimation Theory for Engineers*. Prentice Hall, Inc., 2nd edition, 1994.

[39] R. S. Strichartz. *The Way of Analysis*. Jones and Bartlett Publishers, 2000.

[40] S. Strogatz. *Sync: The Emerging Science of Spontaneous Order*. Theia, 2003.

[41] C. Vanvreeswijk and L. F. Abbott. Self-Sustained Firing in Populations of Integrate-and-Fire Neurons. *SIAM Journal on Applied Mathematics*, 53(1):253-264, 1993.

[42] T. J. Walker. Acoustic Synchrony: Two Mechanisms in the Snowy Tree Cricket. *Science*, 166:891-894, 1969.

[43] B. Warneke, M. Last, B. Liebowitz, and K. S. J. Pister. Smart Dust: Communicating with a Cubic-Millimeter Computer. *IEEE Computer Mag.*, 34(1):44–51, 2001.

PLACE PHOTO HERE

An-swol Hu was born in New York State and grew up in California. He received his B.S. in Electrical Engineering from Stanford University in 2002. Currently he is a Ph.D. candidate in the School of Electrical and Computer Engineering at Cornell University. His research interests include applied statistics and statistical signal processing, with applications to sensor networks.

PLACE PHOTO HERE

Sergio D. Servetto was born in Argentina, on January 18, 1968. He received a Licenciatura en Informatica from Universidad Nacional de La Plata (UNLP, Argentina) in 1992, and the M.Sc. degree in Electrical Engineering and the Ph.D. degree in Computer Science from the University of Illinois at Urbana-Champaign (UIUC), in 1996 and 1999. Between 1999 and 2001, he worked at the Ecole Polytechnique Federale de Lausanne (EPFL), Lausanne, Switzerland. Since Fall 2001, he has been an Assistant Professor in the School of Electrical and Computer Engineering at Cornell University, and a member of the field of Applied Mathematics. He was the recipient of the 1998 Ray Ozzie Fellowship, given to "outstanding graduate students in Computer Science," and of the 1999 David J. Kuck Outstanding Thesis Award, for the best doctoral dissertation of the year, both from the Dept. of Computer Science at UIUC. He is also the recipient of a 2003 NSF CAREER Award. His research interests are centered around information theoretic aspects of networked systems, with a current emphasis on problems that arise in the context of large-scale sensor networks.